European Journal of Wood and Wood Products (2024) 82:1879–1899
https://doi.org/10.1007/s00107-024-02131-w

ORIGINAL ARTICLE

Macro- and micromechanical behavior of oil palm wood (*Elaeis guineensis* Jacq.): tensile, compression and bending properties

K. Fruehwald-Koenig[1] · L. Heister[1]

Received: 20 December 2022 / Accepted: 29 July 2024 / Published online: 16 August 2024
© The Author(s) 2024

Abstract
This study investigates the macromechanical and micromechanical behavior of oil palm wood by testing the elastomechanical properties in bending, compression parallel and perpendicular and tension parallel and perpendicular to the vascular bundles of small-size test specimen depending on the position within the trunk, the density and the number of vascular bundles per unit area as well as the plantation site. All properties tested show a much higher exponential increase with the density, following power law relationships with exponents > 1, than common wood species and a significant gradient over both trunk height and cross section. Oil palm wood can be seen as a unidirectional long-fiber-reinforced bio-composite, if vascular bundles are considered as reinforcements (fibers) and parenchymatous ground tissue as matrix. The adapted rule-of-mixture based on the number of vascular bundles per unit area can be confirmed for the density, but not for the tensile properties, because the number of vascular bundles per unit area and share of fibers within the bundles is greater in the periphery than in the trunk central tissue. Furthermore, cell wall thickening over time is more pronounced in the peripheral than in the central tissue and more at the bottom than near the top. Different from small test specimens from common wood species, the compression strength exceeds the tensile strength: $f_{c,0} : f_m : f_{t,0}$ is 1.4 : 2.2–1.2 : 1. The performance indices for minimum weight design by Ashby and coworkers are comparable to that for coconut and date palm wood.

1 Introduction

1.1 Availability of oil palm wood

Oil palms (*Elaeis guineensis* Jacq.) are mainly cultivated in large plantations for palm oil production to be used for food, chemicals, pharmaceuticals and energy. Worldwide, oil palms cover an area of nearly 30 million hectares of which 71% is located in Asia (FAO 2024). Due to declining oil production, the palms are felled after an age of 25+ years and the area is replanted. Like all other biomass, the palm trunks remain on the plantation site for nutrient recycling. This leads to increased insect and fungi populations causing problems for the new palm generation. For various reasons, many regions where oil palms grow currently suffer from a decline in timber harvested from their tropical forests. The average annual total volume of trunks from oil palm plantation clearings amounts to more than 100 million cubic meters (Fruehwald and Koelli 2019). Recent research has explored the potential commercial uses for oil palm wood. In many cases, the wood can be used as a substitute for tropical hardwoods, e.g., in panels (block-boards, flash doors, multi-layer solid wood panels) and construction timber. Appropriate use of the wood requires knowledge of elastomechanical properties and appropriate grading of the lumber.

1.2 Microstructure of oil palm wood

The macromechanical properties of oil palm wood depend on both the properties of its structural components and the features of its microstructure. Regarding the systematics of plants, palms belong to monocotyledons unlike common tree species, which belong to dicotyledons. For the latter, the stems grow in a radial direction and increase in diameter (and height) over time. The cambium (as growing tissue) makes up the stem area between wood and bark. Monocotyledons (such as bamboo) grow only on the top of the plant/tree trunk where the apical meristem is located; no radial

✉ K. Fruehwald-Koenig
katja.fruehwald@th-owl.de

[1] Department for Production Engineering and Wood Technology, OWL University of Applied Sciences and Arts, Campusallee 12, 32657 Lemgo, Germany

cambial growth occurs (apart from some limited increase in diameter achieved through dilatation phenomena). This is important for the structure of the wood tissue. In contrast to common wood species, which have various axial oriented cell types (tracheids, fibers, vessels, parenchyma) and radial oriented wood rays, palms have no radial oriented ray cells, but only lengthwise oriented vascular bundles embedded in parenchymatous ground tissue. Typically, the vascular bundles are composed of fiber, vessel or metaxylem, protoxylem, protophloem or sieve tubes, axial parenchyma, stegmata and companion cells (Lim and Fujii 1997; Tomlinson 1990). The vessels transport water lengthwise from the ground to the apical meristem at the palm top through sclerenchymatous fiber cells forming thick-walled fiber bundles arranged around the vessels serving as main longitudinal load-carrying component determining the mechanical properties. The parenchymatous ground tissue cells contain a high amount of water, sugars and nutrients and have thin walls which easily buckle under load, while, as liquid and solid coupled cell body material, the performance of the living ground tissue can be strengthened by the internal hydrostatic pressure. The parenchyma tissue provides stability to the fibers and transmits loads between them. Figure 1 shows the composition of palm wood. Details on the anatomical characteristics of oil palm wood are given in Lim and Khoo (1986), Tomlinson (1990), Lim and Fujii (1997) and Bakar et al. (2008). Thus, from the structural mechanics point of view, if vascular bundles are considered as the reinforcements (fibers) and ground tissue as the matrix, oil palm wood can be seen as being a unidirectional long-fiber-reinforced biocomposite. Its mechanical properties depend on the mechanical properties of its components and on its microstructural characteristics such as volume fraction and distribution of the sclerenchymatous fibers and the interface properties of the components. However, for numerous palm species (e.g. Tomlinson 1990; Rueggeberg et al. 2008; Rueggeberg et al. 2009; González and Nguyen 2016), the course of the fibrovascular bundles was found to follow a helical path as they ascend the stem before bending rapidly outwards toward a leaf trace at the periphery of the stem. Therefore the composite is not perfectly unidirectional and not fully isotropic in radial and tangential direction.

The number of vascular bundles per area (grade of reinforcement) is high in the outer (peripheral) part of the trunk and decreases gradually towards the inner (central) part and with the height of the trunk (Fathi 2014; Lim and Khoo 1986). Lim and Khoo (1986) showed, that the fiber cells in vascular bundles are shorter in the outer zone than in the center, but in the outer zone they have a greater diameter and thicker cell walls containing higher cellulose content. Also the number of cell wall layers increases from the center to the outer zone because the fibers keep developing their secondary cell wall during their lifetime (cell wall thickening) and followed by a "secondary trunk diameter increase".

1.3 Macromechanical properties of oil palm wood

In the past 35 years, the macromechanical properties of oil palm wood have been widely studied. Because of the property gradient within the cross section and the height of the trunk, all investigations on elastomechanical properties of oil palm wood were performed on small, clear test specimens; only one – Jumaat et al. (2006), who tested trussed rafters from oil palm wood – was performed on bigger test specimens, e.g. construction-size oil palm timber elements. Most literature deals with bending strength (f_m) and stiffness (E_m) (Bakar et al. 1999; Balfas 2006; Darwis et al. 2013; Erwinsyah 2008; Iswanto et al. 2010; Karlinasari et al. 2019; Killmann and Lim 1985; Lim and Gan 2005; Ratanawilai et al. 2006; Srivaro et al. 2018a, b, 2019) and compression strength parallel to the vascular bundles ($f_{c,0}$) (Balfas 2006; Darwis et al. 2013; Erwinsyah 2008; Fathi 2014; Iswanto et al. 2010; Killmann and Lim 1985; Lim and Gan 2005; Ratanawilai et al. 2006; Srivaro et al. 2018a, 2019; Sulaiman et al. 2012), mainly because of the easy preparation of test specimens and test procedures. Young´s modulus in compression parallel to the vascular bundles ($E_{c,0}$) was only determined by Fathi (2014) and Srivaro et al.

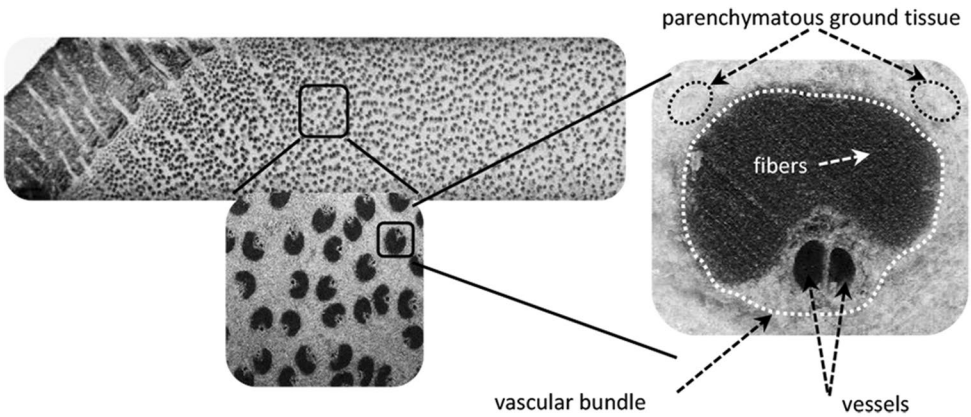


Fig. 1 Cross section of an oil palm board with bulk density differences (left) and illustration of the anatomic structure (right)

(2018a, 2019). Compression strength perpendicular to the vascular bundles ($f_{c,90}$) was only determined by Killmann and Lim (1985) and Srivaro et al. (2018a). Perhaps because of the difficulties involved in preparing the test specimens and test procedure, only two investigations were found on the tension strength parallel to the vascular bundles ($f_{t,0}$) (Erwinsyah 2008; Iswanto et al. 2010) and perpendicular to the vascular bundles ($f_{t,90}$) (Erwinsyah 2008; Ratanawilai et al. 2006), but no property values were found on the Young´s modulus in tension ($E_{t,0}$ and $E_{t,90}$). The literature is limited on the systematic and comprehensive determination of the mechanical properties of oil palm wood (Erwinsyah 2008; Iswanto et al. 2010; Ratanawilai et al. 2006; Srivaro et al. 2018a), most investigations concentrate on one or only a few properties. Many previous results were determined on a small quantity of specimen, which is problematic especially considering the wide range in density (and therefore also widely varying properties). Also, the studies often examined very different trunk areas (regarding cross-section and height in the palm) and thus studied very different density ranges (e.g., Ratanawilai et al. 2006, Erwinsyah 2008, and Tufashi 2013) used mostly test material from the peripheral of the trunk with higher density; Srivaro et al. (2018a) used test specimens from sections with comparable lower density), therefore the results of the various investigations are hardly comparable with each other. Even at the same density, the origin of the height and the age of the trunk have a considerable influence on the macromechanical properties of the oil palm wood (Killmann and Lim 1985). Therefore, most authors (e.g. Erwinsyah 2008) modeled the mechanical properties depending on the location within the trunk in regard to the cross section and the trunk height (mechanical properties = f(cross section, height)), and some (e.g. Darwis et al. 2013, Fathi 2014) modeled depending on the number of vascular bundles per unit area (mechanical properties = f(# VB per area)) or area proportion of vascular bundles (mechanical properties = f(VB area fraction)). The position within the cross section at a certain trunk height influences the mechanical properties because of the rising number of vascular bundles per unit area (and area proportion of vascular bundles) from the center to the periphery, therefore the density and the mechanical properties increase from the center to the periphery of the cross section (e.g. Darwis et al. 2013; Erwinsyah 2008; Fathi 2014; Killmann and Lim 1985; Srivaro et al. 2018b). The position over the trunk height influences the mechanical properties because of the cell wall thickening during the cell wall lifetime (Lim and Khoo 1986). With rising height from the bottom to the top of the trunk, the number of vascular bundles per unit area increases while the density and mechanical properties decrease. This is because younger cells have different properties than mature cells due to their incomplete lignification and the cell wall thickening process (the number of cell wall layers and therefore the density of the vascular bundles decrease from the bottom to the top) (Darwis et al. 2013; Fathi 2014; Killmann and Lim 1985; Lim and Khoo 1986). According to Gibson et al. (2010) and González and Nguyen (2016), the anatomical structure reflects an optimized palm fibrovascular development resulting from the natural adaption of the material to resist varying conditions of external forces, e.g. gravity (biomass), wind, rain, water, and the leaf formation pattern to obtain maximum sunlight; furthermore the age of the oil palm influences the anatomical structure. A serious drawback of the existing studies is that the work on elastomechanical properties has not taken into account the differences between different trunks and between different plantation sites or regions of origin.

1.4 Research question and assumptions

Precise studies on the micromechanical properties of oil palm vascular bundles and parenchymatous ground tissue with respect to its fiber-reinforced composite structure, however, have not been sufficiently reported. Therefore, this study aims to investigate the macromechanical and micromechanical behavior of oil palm wood by testing the "apparent" macromechanical properties, namely strength and stiffness. The investigation involves the extensive testing of numerous specimens extracted from various trunks originating from two distinct plantation sites. Additionally, specimens are collected from various positions along cross sections and at different heights within the trunk. The corresponding number of vascular bundles per unit area and bulk density are determined and correlated to the macromechanical properties. The various material properties are compared in between and with common wood species depending on the density and number of vascular bundles per unit area separately for the two plantation sites. The following considerations are based on the hypothesis that oil palm wood (1) is a unidirectional, long-fiber-reinforced composite (the helically wound fiber-reinforced circular oil palm trunk cylinder is neglected), (2) is orthotropic and (3) has different "apparent" properties in tension and compression as do most composite materials. The basic restrictions for composite materials shown in Table 1 are assumed valid for oil palm wood. Therefore, the elastic properties of orthotropic materials (3 elastic moduli (E), 3 shear moduli (G) and 6 Poisson´s ratio (ν)) and the six strength properties in tension ($f_{t,0}$, $f_{t,90}$), compression ($f_{c,0}$, $f_{c,90}$) and shear ($f_{v,0}$ and $f_{v,90}$) should be determined. In this paper, the properties in compression and tension parallel and transverse to the vascular bundles and the bending properties parallel to the vascular bundles are characterized. The shear properties are not

Table 1 Basic restrictions for composite materials according to Jones (1999) adapted for oil palm wood

The composite is	initially stress free
	linearly elastic
	macroscopically homogeneous
	macroscopically orthotropic
The fibers (fiber caps / vascular bundles) are	homogeneous
	linear elastic
	isotropic
	regularly spaced
	perfectly aligned
	perfectly bonded
The matrix (parenchymatous ground tissue) is	homogeneous
	linear elastic
	isotropic
	void-free

covered in this investigation but will be addressed, along with an examination of the elastic constants, in a second paper.

When the radial thickness of a specimen is a few millimeters only, the vascular bundles can be considered as being uniformly distributed (regularly spaced) within the test specimen. Normally, fibers, and therefore vascular bundles, have high strength and stiffness while ground tissue has low strength and stiffness and high capability of deformation. This study found (cf. Chapter 4.2) that in the tensile stress (σ) - strain (ε) curve of oil palm wood (tested parallel to the vascular bundles), the part from the beginning of loading to the breaking point was almost linear. Therefore, in view of mechanical behavior, the oil palm wood can be simplified as a composite of parallel connection models composed of two elements, i.e., vascular bundles and parenchymatous ground tissue. It is assumed that under load, vascular bundles and ground tissue have the same deformation.

In materials science, the general rule of mixtures is a weighted mean used to predict various properties (elastic modulus, mass density, ultimate tensile strength, thermal conductivity, electrical conductivity) of a composite material made up of continuous and unidirectional fibers. The Voigt model is used for axial loading and the Reuss model for transverse loading. According to the Voigt model, the density, tensile strength and the elastic modulus parallel to the vascular bundles should be a linear function of the volume fraction of the fibers (V_{fiber}). Therefore, a linear function between the tensile strength parallel ($f_{t,0}$) and the density (ρ) respectively the Young´s modulus parallel ($E_{t,0}$) and the density (ρ) should exist.

2 Material

Material from two locations was used. Material origin 1: For compression II and ⊥, tension II and bending tests, 14 palms were felled at an age of 33 years on a plantation located in South Peninsular Malaysia near the city of Kluang in Johor (altitude of 40 m, tropical climate throughout the year with an annual mean temperature of 26 °C and an average of 2438 mm precipitation per year) (Koelli 2016). The subspecies of the palms could not be identified precisely, but according to Koelli (2016) it can be assumed that the palms were from picifera species or a subspecies between picifera and tenera due to the appearance of their fruit. The trunks were cut to four sections along the trunk height (0.5–3.25 m, 3.25–6.0 m, 6.0–8.75 m and 8.75–11.5 m) and imported in frozen state at -10 °C to Germany and sawn in two sawmills (bandsaw with log carriage and circular saw) into un-edged and square-edged boards (dimensions in mm: 1950 × 130…300 × 23…60). The boards were kiln dried in a laboratory kiln at the University of Hamburg (temperature < 85 °C) (Harnisch 2016).

Material origin 2: For compression II and ⊥, locally compression ⊥ ($f_{lc,90}$) and tension II and ⊥, 150 oil palms (*Elaeis guineensis* Jacq.*var. pisifera*) were felled at an age of 30 years on a plantation located in Johor, South Peninsular Malaysia. From 100 palms, the lower section of 2.8 m (1–4 m trunk height) and from 50 palms, the first two sections of 2.8 m (1–4 m and 4–7 m height) were sawn at the Forest Research Institute Malaysia (FRIM) on a bandsaw with log carriage into partly square-edged boards (27 and 50 mm thickness). To prevent mold growth during storage and transport of the wet wood as well as the kiln drying, the boards were dipped in acetic acid (10% concentration) for 2–5 min. The material was kiln dried at very low temperature below 70 °C in an industrial kiln and imported in dry state to Germany (Koelli 2018).

From the material, the test specimens compiled in Table 2 were produced in accordance with the specifications in the corresponding standards. An attempt was made to obtain the most uniform possible distribution of the specimens over the entire density spectrum, but due to the available material it was not possible to guarantee a uniform distribution of the specimens over the trunk height and cross section. In order to investigate the influence of the specimen height on the compressive strength parallel to the vascular bundles ($f_{c,0}$), three different specimen heights were investigated for material origin 2. For testing $f_{c,90}$ no distinction was made between the radial and tangential direction due to Killmann and Lim (1985). In order to obtain a uniform density over the entire test specimen, the specimens for $f_{lc,90}$ and $f_{t,90}$ according to ASTM D143 (2014) were built up of three 17 mm layers (glued with 1 K-PUR, gluing line orthogonal to the

Table 2 Overview of test specimens

Test	Standard	Dimension	Number of specimens tested	Material origin
Compression II ($f_{c,0}$)	DIN 52185 (1976)	20×20×30 mm³	75	1
		17×17×26 mm³	82	2
		17×17×39 mm³	76	
		17×17×51 mm³	74	
Compression ⊥ ($f_{c,90}$)	DIN 52192 (1979)	20×20×60 mm³	79	1
		17×17×26 mm³	52	2
		17×17×39 mm³	42	
		17×17×51 mm³	35	
Local compression ⊥ ($f_{lc,90}$)	ASTM D143 (2014)	50×150[2)] x 50 mm³	73	2
Tension II ($f_{t,0}$, $E_{t,0}$)	DIN 52188 (1979)	6[1)] x 20×470 mm³	109	1
			92	2
Tension ⊥ ($f_{t,90}$)	ASTM D143 (2014)	25[1)] x 50×60 mm³	102	2
	EN 319 (1993 (D))	50×50×14…20 mm³	40	2
Bending (f_m, E_m)	DIN 52186 (1978)	22×22×380 mm³	647	1
		18×18×320 mm³	28	

[1)] tested cross section

[2)] 50×50 mm² tested cross section

testing force). The specimens for tensile test II had a thickness of 12 mm instead of 15 mm due to the limited spacing between the clamping jaws of the wedge specimen holders. Due to the expected low compression strength perpendicular to the vascular bundles, beech veneer plywood was used to increase the clamping area in order to avoid compression failure of the tensile test specimen between the clamping jaws. Notwithstanding all other tests, the investigation of the bending properties depending on the location within the trunk (Chap. 4) was performed only on one palm stem. Due to drying defects, no test specimen could be processed from the third trunk section (6.0–8.75 m). The dimensions of the bending test specimens deviate minimally from DIN 52186 (1978): 90% of the specimens had a dimension of 22×22×380 mm³ and 10% of 18×18×320 mm³. Before testing, all test specimens were stored to constant weight in standard climate 20 °C, 65% relative humidity (DIN 50014-20/65 – 1 according to DIN 50014 (2018)).

3 Methods

Testing of the various strength and elasticity values was carried out using the universal testing machine Zwick Z020 with a 2.5 kN respectively 20.0 kN load cell in accordance with the standardized test methods for testing the mechanical properties of wood (Table 2), because no special test methods and standards are currently available for oil palm wood. The strain measurements in testing compression II and ⊥, local compression ⊥ and tension ⊥ were not carried out by means of an attached length-measuring device but through the movable vertical crosshead, which measures the distance between the upper and lower compression plate. However, Kipp (2022) showed on different wood species (among others oil palm wood) and specimen geometries that distance measurement through the movement of the vertical crosshead leads to an overestimation of the strain and therefore incorrect determination of Young´s modulus, that´s why the results for $E_{c,0}$, $E_{c,90}$, $E_{lc,90}$ and $E_{t,90}$ are not included in Chap. 4. The compression test II was carried out according to DIN 52185 (1976). The compression test ⊥ was carried out according to DIN 52192 (1979) with loading over the entire specimen surface, which differs from ISO 3132 (1975) used by Killmann and Lim (1985) in the specimen geometry, and the proportional limit ($f_{c,90}$) was determined according to ISO 3132 (1975). The local compression test ⊥ with loading over the 1/3 specimen surface was carried out according to ASTM D143 (2014) and the proportional limit ($f_{lc,90}$) determined at 2.5 mm displacement according to ISO 3132 (1975). The tensile test ⊥ was carried out according to ASTM D143 (2014) respectively EN 319 (1993 (D)). The tensile test II was carried out according to DIN 52188 (1979); the measurement of the elongation was done by means of a manually mounted incremental piecing receiver (digiClip) from Zwick. The three-point bending test was performed according to DIN 52186 (1978), the test direction (radial, tangential or a mixture thereof) was chosen randomly. For each test specimen, the density was determined according to DIN 52182 (1976). The density of the tensile specimen was determined on the rectangular bars prior to the curve milling of the specimens, since the determination of the density on a contour-milled, two-dimensional specimen would have led to inaccuracies. Due to the storage in the standard climate up to constant mass of the test specimen, the moisture content was determined only at random after the destructive test using oven dry test. For each bending test specimen, the number of vascular bundles per unit area was determined after the destructive test close to the fracture area. The cross

section was captured by means of HD photography, using Photoshop Image Program, and contrast filters were used to illustrate shades, colour differences in the parenchyma and detached vascular bundles. All countable vascular bundles were visually recorded.

4 Results and discussion

For the various properties, various regression models (strength and stiffness as a function of the density, strength as a function of the stiffness), including linear and nonlinear relationships, with their associated R-squared (R^2) were determined. The power law relationship gave a better fit for strength and stiffness with the density, showing similar or higher R^2 compared with those obtained from linear relationship. Similar findings are reported by Rich (1987b) and Srivaro et al. (2018a, b). Therefore, in this study, the power law relationship is used to plot all experimental results of elastomechanical properties. The non-uniform distribution of the specimens over trunk height and cross section and from various trunks (cf. Chapter 2) are influencing the results.

4.1 Density and number of vascular bundles per area

The values of the density (ρ) of all test specimens range from 140 to 660 kg/m³, in regard to the density the material is comparable to that used by Killmann and Lim (1985) (ρ_0 = 220…550 kg/m³), Gan et al. (2001) (basic density = 150…635 kg/m³) and Balfas (2006) ($\rho_{air-dry}$ = 210…670 kg/m³). In comparison, Erwinsyah (2008) (ρ_{12} = 160…430 kg/m³) and Srivaro et al. (2018a) (ρ_{12} = 222…404 kg/m³) tested material of lower and Ratanawilai et al. (2006) (ρ_{12} = 380…510 kg/m³), Tufashi (2013) (ρ_{12} = 330…620 kg/m³) and Bakar et al. (2013) (290…610 kg/m³) material of higher density.

The plot of the density of the bending specimens (ρ) related to their number of vascular bundles per area is shown in Fig. 2. The density is increasing with the number of vascular bundles per area in cm² by linear regression independent of the trunk height (R^2 = 0.76), because in the multiple linear regression model the inclusion of the trunk height did not significantly enhance the explanatory power of the regression equation ($\Delta R^2_{adj.}$ = 0.004). The linear relationship between the density and the number of vascular bundles per area confirms the adapted rule-of-mixture, which is based on the assumption of a constant vascular bundle diameter over the entire trunk. However, according to Fathi (2014) and Lim and Khoo (1986), the vascular bundle diameter is constant over the cross section, but decreases with increasing height within the trunk. Therefore, the usual rule-of-mixture based on the volume fraction of the vascular bundles is confirmed for the individual heights within the trunk, but a small influence of the height can not be excluded. The intercept of the relationship gives an estimate of the parenchyma density with $\rho_{parenchyma} \approx 117$ kg/m³.

4.2 Tensile tests parallel to the vascular bundles

The plot of the tensile strength parallel to the vascular bundles ($f_{t,0}$) and the Young´s modulus in tension ($E_{t,0}$) related to density is shown in Fig. 3. The values of $f_{t,0}$ are dependent on the height within the trunk and range from 1.9 to 47.0 MPa, do not differ for the two material origins and are comparable to those of Erwinsyah (2008) (6.2…39.3 MPa for test specimen only from peripheral zone) and Iswanto

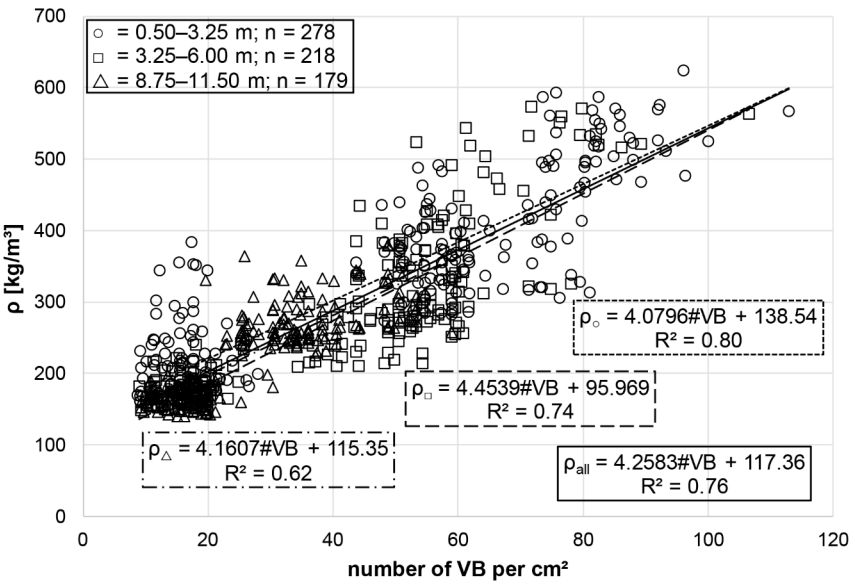


Fig. 2 Density (ρ) (measured on bending test specimens) plotted against the number of vascular bundles per area; the intercept of the relationship gives an estimate of the parenchyma density

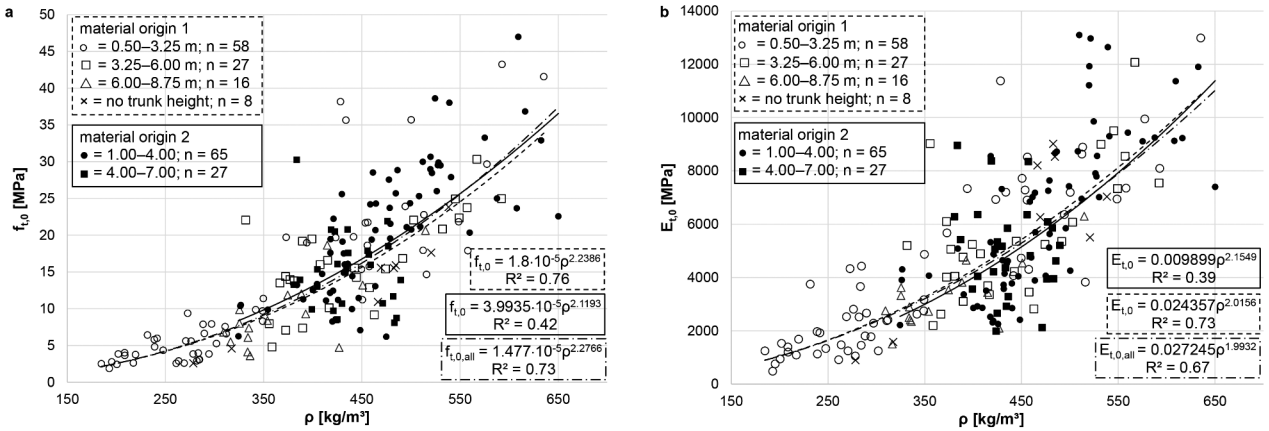


Fig. 3 Tensile properties parallel to the vascular bundles plotted against the density (ρ); **a** tensile strength ($f_{t,0}$) and **b** Young´s modulus in tension ($E_{t,0}$); for 8 test specimens, the height within the trunk could not be determined (marked with x)

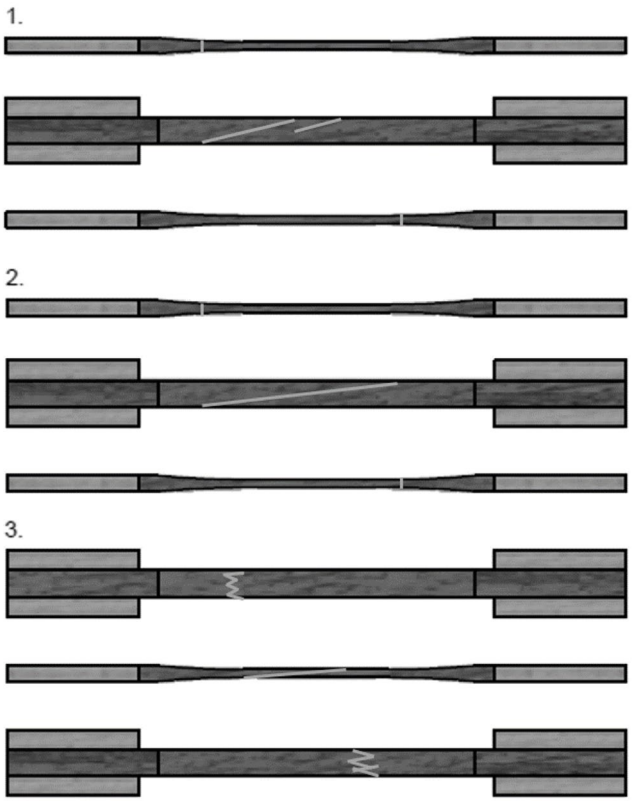


Fig. 4 Fracture patterns after the tensile test parallel to the vascular bundles (**1**) double failure over the width, (**2**) single failure over the width, (**3**) single failure over the thickness

et al. (2010) (10.3…33.8 MPa). The values for the Young´s modulus in tension ($E_{t,0}$) are dependent on the height within the trunk and range from 488 to 13,102 MPa, but do not differ for the two material origins. Tensile strength and Young´s modulus are increasing with increasing density by power law equation ($R^2 = 0.73$ respectively $R^2 = 0.67$). The exponents for $f_{t,0}$ and $E_{t,0}$ are approximately 2.2766, respectively 1.9932 and therefore, based on the linear relationship between density and number of vascular bundles per area (Chap. 4.1), the adapted rule of mixture cannot be confirmed (because then a linear relationship or an exponent close to 1 would have had to be observed). As for many fiber-reinforced composite materials, the stress-strain behavior of the tensile test parallel is linear from zero load to the ultimate or fracture load and showing brittle rupture, this is typical for most wood species in tension as well. Tensile failure of a fibrous composite loaded in a direction parallel to the set of uniaxial reinforcing fibers would be fiber fracture, described in detail in Dow and Rosen (1965). With an angle between the fiber direction and the direction of the applied tensile stress, according to Kelly and Davies (1965) failure can occur in general (in the order of rising angle) by (a) flow of the matrix parallel to the fibers until the fibers fail, (b) failure of the matrix in shear on a plane parallel to the fibers and (c) failure of the matrix by flow transverse to the fibers. Figure 4 shows the observed three tension fracture patterns with all failures due to an angle between the vascular bundles and the direction of the applied tensile stress. No difference is observed between the two material origins: 57% of the specimens broke over the thickness (fracture no. 3), 23% over the width (single fracture) (fracture no. 2) and 19% over the width (double fracture) (fracture no. 1). The macroscopic fracture patterns differ significantly from those for softwoods and hardwoods according to Bodig and Jayne (1982) (splintering tension, combined tension and shear, shear, brittle tension) or bamboo according to Shao and Wang (2018) (brittle tension, uneven tension, splintering tension). The angle between direction of the vascular bundles and direction of the applied tensile stress results in strength values measured too low. Because of the helical orientation of the bundles with deviations in radial direction (Tomlinson 1990; Rueggeberg et al. 2008, 2009; González

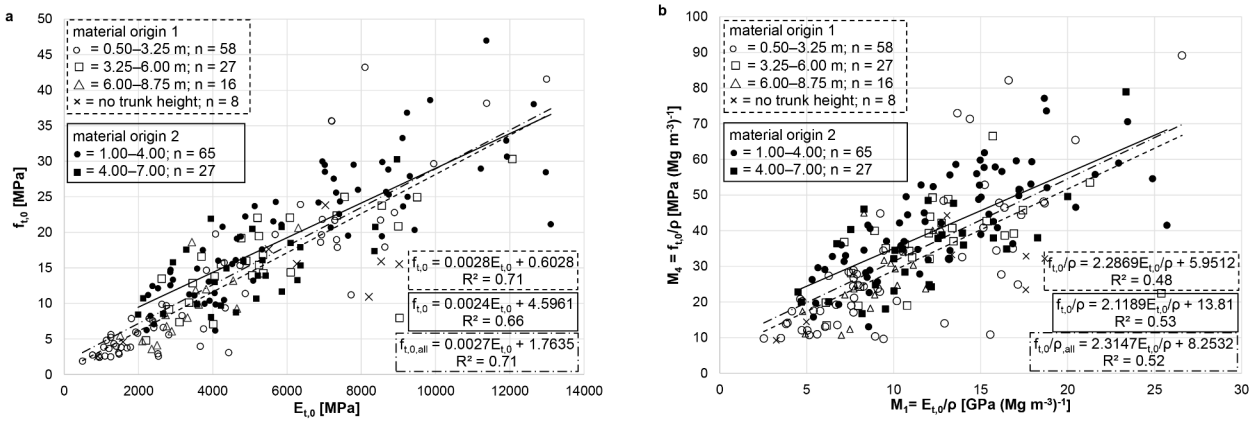


Fig. 5 Relationship between tensile strength ($\mathbf{f}_{t,0}$) and stiffness ($\mathbf{E}_{t,0}$) parallel to the vascular bundles; **a** absolute values and **b** specific values resp. performance indices; for 8 test specimens, the height within the trunk could not be determined (marked with x)

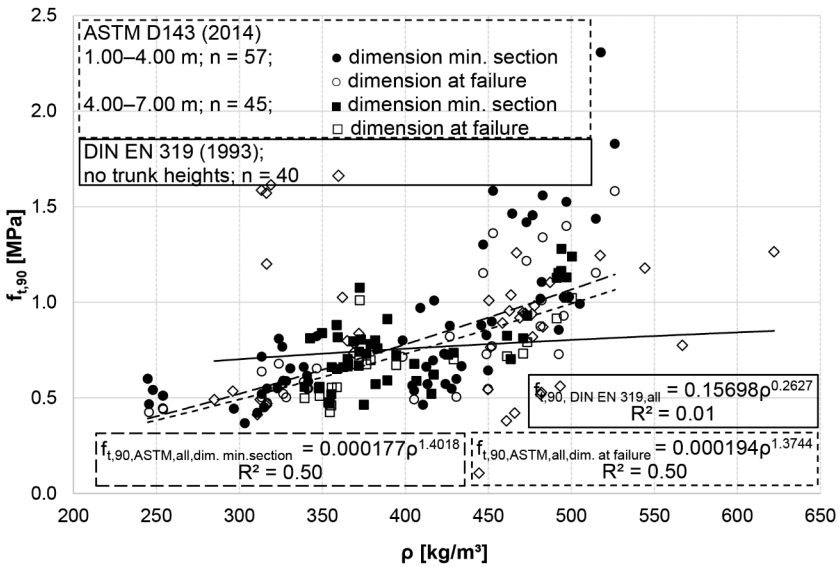


Fig. 6 Tensile strength perpendicular to the vascular bundles ($f_{t,90}$) plotted against the density (ρ)

and Nguyen 2016), it is not possible to process small (that regular spaced vascular bundles) test specimens with perfectly aligned vascular bundles along the axis of the test specimens.

Fig 5a shows that the $f_{t,0}$ is quite strongly related to $E_{t,0}$, showing $R^2 = 0.71$, which indicates that $f_{t,0}$ can be predicted from the known $E_{t,0}$ value. In terms of structural performance, the specific tensile strength ($M_4 = f_{t,0}/\rho$) and specific Young´s modulus ($M_1 = E_{t,0}/\rho$) parallel to the vascular bundles shall be considered, shown in Fig. 5b. Because of the power law relationship between tensile strength, respectively Young´s modulus and density, the performance indices for minimum weight design by Ashby et al. (1995) calculated for oil palm wood rise with the density (Table 3). Assumed densities between 200…600 kg/m³ for oil palm wood result for tensile members in calculated $M_4 = f_{t,0}/\rho = 8.8…36.0$ MPa $(\text{Mg m}^{-3})^{-1}$ (a tie under uniaxial load), the strength-density performance indices M_4 – M_6 (M_4 tie under uniaxial load, M_5 beam in flexure, M_6 plate in flexure) are much lower than that of small, clear wood test specimens, high-density oil palm wood is in the range of low-grade softwood lamellas of structural size (Table 3). $M_1 = E_{t,0}/\rho = 5.2…15.3$ GPa $(\text{Mg m}^{-3})^{-1}$ (tie in tension). The performance index for elastic design $M_8 = f_{t,0}/E_{t,0}$ to allow large, recoverable deformation is almost constant for all densities of oil palm wood with $M_8 = 0.0017…0.0024$ and lower than that for small, clear wood test specimens, but in the range of structural size softwood lamellas (Table 3)

Assuming that vascular bundles all have the same strength (which is proved wrong by Fathi (2014) $f_{t,0,\text{fiber}} = 58…225$ MPa and $E_{t,0,\text{fiber}} = 2{,}385…16{,}973$ MPa, depending on the cross section and height of the trunk) and are relative brittle in comparison to the parenchymatous ground tissue (note that no stress-strain curves for vascular bundles

Table 3 Performance indices for minimum weight design according to Ashby et al. (1995)

Material	Modulus-density performance indices			Strength-density performance indices			Modulus-strength performance index	Source of original / basic data
	$M_1 = E/\rho$ [GPa (Mg $m^{-3})^{-1}$]	$M_2 = E^{1/2}/\rho$ [$GPa^{1/2}$ (Mg $m^{-3})^{-1}$]	$M_3 = E^{1/3}/\rho$ [$GPa^{1/3}$ (Mg $m^{-3})^{-1}$]*	$M_4 = \sigma_f/\rho$ [MPa (Mg $m^{-3})^{-1}$]	$M_5 = \sigma_f^{2/3}/\rho$ [$MPa^{2/3}$ (Mg $m^{-3})^{-1}$]	$M_6 = \sigma_f^{1/2}/\rho$ [$MPa^{1/2}$ (Mg $m^{-3})^{-1}$]*	$M_8 = \sigma_f/E$ [-]	
	tie under uniaxial load	beam in flexure; column buckling	plate in flexure	tie under uniaxial load	beam in flexure	plate in flexure	allow large, recoverable deformations	
Oil palm wood	5.2…15.3[a]	5.1…15.2[a]	5.1…3.5[a]	8.8…36.0[a] 20.3…78.4[b]	7.3…12.9[a] 12.7…21.7[b]	6.6…7.7[a] 10.1…11.4[b]	0.0017…0.0024[a]	own results
Coconut palm wood	9.4…14.5[b]	4.6…5.6[b]	3.1…4.5[b]	61…86[b]	23.0…22.1[b]	14.1…11.3[b]	0.0058…0.0072[b]	Sulc (1985)
Date palm wood				33.5…47.2[b]	15.5…13.5[b]	10.5…8.2[b]		Elkhal et al. (2022)
Acacia mangium				69[b]	19.6[b]	10.5[b]		Tan (1979), cit. in Peh and Khoo (1984)
Paraserianthes [Albizia] *falcataria*				79.5[b]	26.7[b]	15.4[b]		Bolza and Kloot (1966)
Hevea brasiliensis				136…140[a] 57…71[b]	32.0…29.9[a] 18.0…19.1[b]	15.6…13.8[a] 10.1…9.9[b]	0.0083…0,0111[ac] 0.0035…0.0057[bc]	Wagenfuehr (2000)
Tectona grandis				169[a] 85[b]	34.8[a] 22.0[b]	15.8[a] 11.2[b]	0.0088[ac] 0.0045[bc]	DIN 68364 (2003)
Softwood lamellas T8…T30 (structural size)	20.0…30.6[a]	7.5…7.9[a]	5.5…4.8[a]	27.6…69.8[ad] 55.2…70.7[bd]	13.8…22.5[ad] 21.9…23.0[bd]	9.8…12.7[ad] 13.8…13.1[bd]	0.0017…0.0028[acd] 0.0034…0.0028 [bcd]	EN 338 (2016 (D))

[a] based on tensile tests

[b] based on compression tests

[c] E based on bending tests

[d] calculation based on the 5th quantile

* values are calculated based on the longitudinal strength, therefore they are not representative of the efficiency of a strong plate in bending which requires isotropic strength

and parenchymatous ground tissue are available in the literature yet), according to Kelly and Davies (1965), if V_f is less than $V_{fminimum}$, the composite material strength is controlled by the matrix deformation and is actually less than the matrix strength. When V_f is greater than $V_{fminimum}$, but less than $V_{fcritical}$, the composite material strength is controlled by the fiber deformation, but the composite material strength is still less than the inherent matrix strength. Only when V_f exceeds $V_{fcritical}$, the composite material gains strength from having fiber reinforcement (based on the rule of mixtures with linear correlation between $f_{t,0}$ and V_f). To calculate $V_{fcritical}$, $V_{fminimum}$ and the strength of the composite material, beside the fiber volume fraction (V_f), the maximum fiber tensile stress ($f_{t,0,fiber} = 58…225$ MPa, depending on the cross section and height of the trunk in Fathi (2014)), the maximum matrix tensile stress (not known for parenchmatous ground tissue yet), the matrix stress at a matrix strain equal to the maximum tensile strain of the fibers (not known for parenchmatous ground tissue yet) are necessary. A calculation method for fibers with statistical strength distribution is described by Rosen (1964). Rosen´s results lead to non-linear results, but are usually, according to Dow and Rosen (1965), close to the rule-of-mixture expressions.

The apparent Young´s modulus of the composite material in the direction of the fibers can be calculated according to the rule-of-mixtures as lower bound (if the Young´s modulus of the parenchymatous ground tissue would be known) (Jones 1999). If the fiber modulus is assumed many times higher the matrix modulus, the fiber modulus dominates the composite modulus.

4.3 Tensile tests perpendicular to the vascular bundles

The plot of the tensile strength perpendicular to the vascular bundles ($f_{t,90}$) related to density is shown in Fig. 6. The values range from 0.4 to 2.3 MPa and are in the same range for ASTM D143 (2014) and EN 319 (1993 (D)). They are comparable to those of Ratanawilai et al. (2006) (0.6…1.0 MPa) and are much above those of Erwinsyah (2008) (0.3…0.4 MPa at 3 to 7 m trunk height). The tensile strength according to ASTM D143 (2014) shows a moderate correlation to the density of the whole test specimen ($R^2 = 0.50$), whereas the tensile strength according to EN 319 (1993 (D)) shows no correlation to the density ($R^2 = 0.01$). This is induced by the density gradient within the single test specimen, the failure took place in the zone with the lowest density (Fig. 7), whereas only the density of the whole test specimen was determined. Therefore, the diagramed density in Fig. 6 is higher than the density in the failure zone (at least in the failure starting zone), according to the density-gradient over the cross section in Koelli (2016) this difference increases with the density. Many specimens in the test according to ASTM D143 (2014) showed a failure outside the minimum cross section of 25 × 50 mm (Fig. 7, middle). Therefore, $f_{t,90,ASTM\ D143}$ was calculated two times: based on the dimension at the minimal cross section (25 × 50 mm) ($f_{t,90,\bullet}$ and $f_{t,90,\blacksquare}$ in Fig. 6) and at the failure´s cross section ($f_{t,90,\circ}$ and $f_{t,90,\square}$), which leads to a slightly lower tensile strength ⊥. If the failure is outside the minimum cross section, the "real" tensile strength at minimal cross section is higher than the determined value based on the dimension at the minimal cross section (25 × 50 mm). In contrast to Ratanawilai et al. (2006) and Erwinsyah (2008), the tensile strength perpendicular to the vascular bundles seems only slightly influenced by the height because only the lower 1…7 m within the trunks were investigated.

4.4 Compression tests parallel to the vascular bundles

The plot of the compression strength parallel to the vascular bundles ($f_{c,0}$) related to density is shown in Fig. 8. The values of the compression strength ($f_{c,0}$) are dependent on the height within the trunk and range from 3.1 to 64.4 MPa, do not differ for the two material origins and are comparable to those of Lim and Gan (2005) (13.0…31.4…38.1 MPa for $\rho \leq 350$ … 350–500 … > 500 kg/m³), Balfas (2006) (16.9…53.4 MPa for $\rho_{air-dry} = 330…670$ kg/m³), Killmann and Lim (1985) (5…25 MPa) and Ratanawilai et al. (2006) (20.7…30.2 MPa for $\rho_{12} = 380…510$ kg/m³) and above those of Erwinsyah (2008) (16.7…23.2 MPa for test specimens

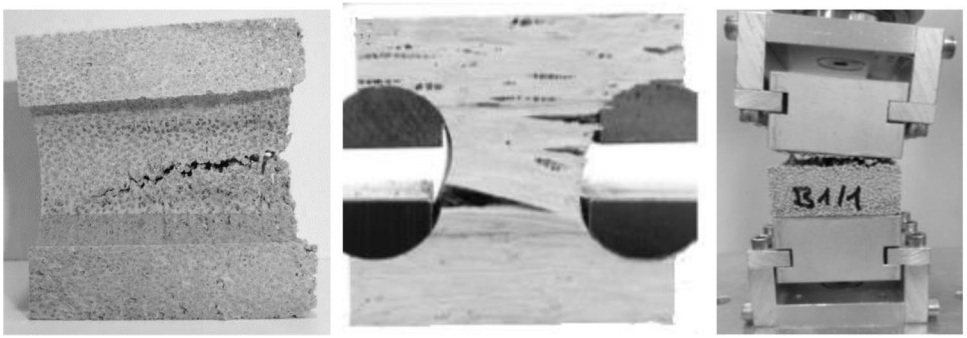


Fig. 7 Fracture patterns after the tensile test perpendicular to the vascular bundles, left and middle: specimen according to ASTM D143 (2014), right: specimen according to EN 319 (1993 (D))

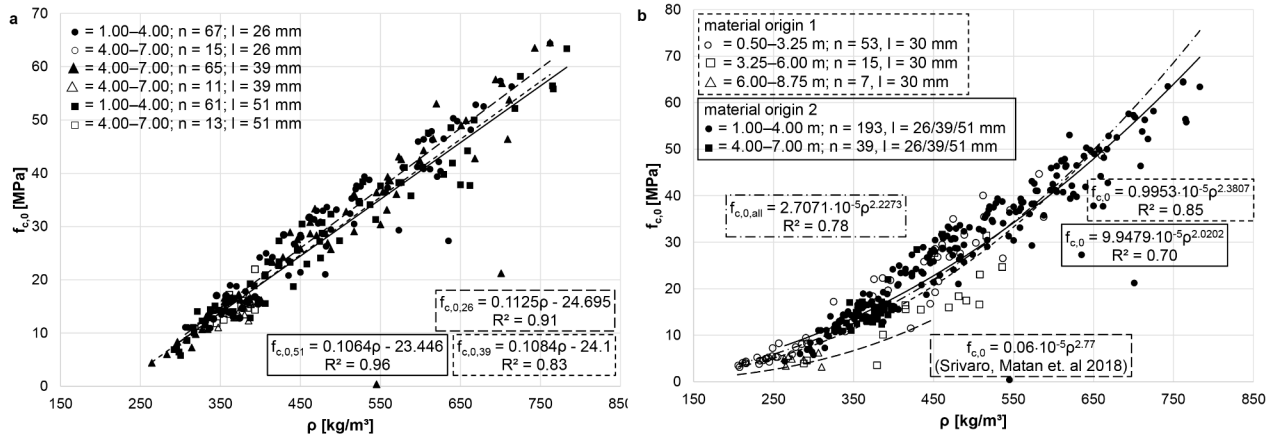


Fig. 8 Compression strength parallel to the vascular bundles ($\mathbf{f}_{c,0}$) plotted against the density (ρ); **a** for material origin 2 differentiated according to the specimen height and **b** for both material origins, not differentiated according to the specimen height

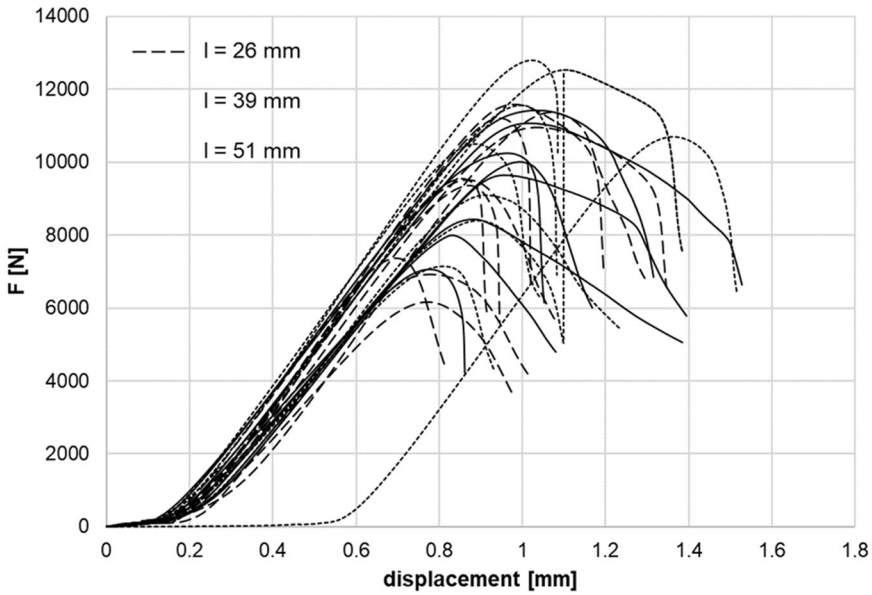


Fig. 9 Force-displacement curves of specimens from the same board with various lengths loaded in compression parallel to the vascular bundles

only from peripheral zone), Fathi (2014) (4.4…27.6 MPa), Iswanto et al. (2010) (3.8…13.9 MPa) and Srivaro et al. (2018a) (1.3…10.2 MPa). The compression strength increases with increasing density by the power law equation ($R^2 = 0.78$). The exponent for $f_{c,0}$ is 2.2273 and only slightly below that of Srivaro et al. (2018a) (2.77) for oil palm wood, but much higher than that of Fathi (2014) (1.0) and that for common wood species (modelled exponent 1.0 according to Easterling et al. (1982) and Gibson and Ashby (1999); experimentally derived exponent 1.0 according to Markwardt and Wilson (1935) and for softwoods 0.97, respectively hardwoods 0.89, according to Kretschmann (2010)). The stress-strain behavior of the compression test parallel is linear from zero load to the ultimate or fracture load with brittle rupture (Fig. 9), this is typical for fiber-reinforced composites and very different from softwoods and hardwoods with ductile behavior and no fracture. Figure 10 exemplifies the failure mode on two samples of oil palm wood during the compression test parallel to the vascular bundles. The vascular bundles are buckling; the buckling failure of the individual vascular bundles could be heard and is shown afterwards microscopically (Fig. 11a) and in a 3D-reconstruction (Fig. 11b) because the parenchyma next to the fibers is too weak (extremely thin cell walls) to stabilize the fibers / vascular bundles. This is in line with the literature for composite materials with low modulus matrix, Dow and Gruntfest (1960), cit. in Dow and Rosen (1965) describe that the mode of failure appears to be fiber buckling within the restraint of the matrix material, called "microbuckling" by Greszczuk (1975). Greszczuk (1975) distinguishes two possible buckling patterns: (1) "transverse" or "extensional" buckling mode (if the composite



Fig. 10 Two test specimens during the compression test parallel to the vascular bundles: vascular bundles are buckling

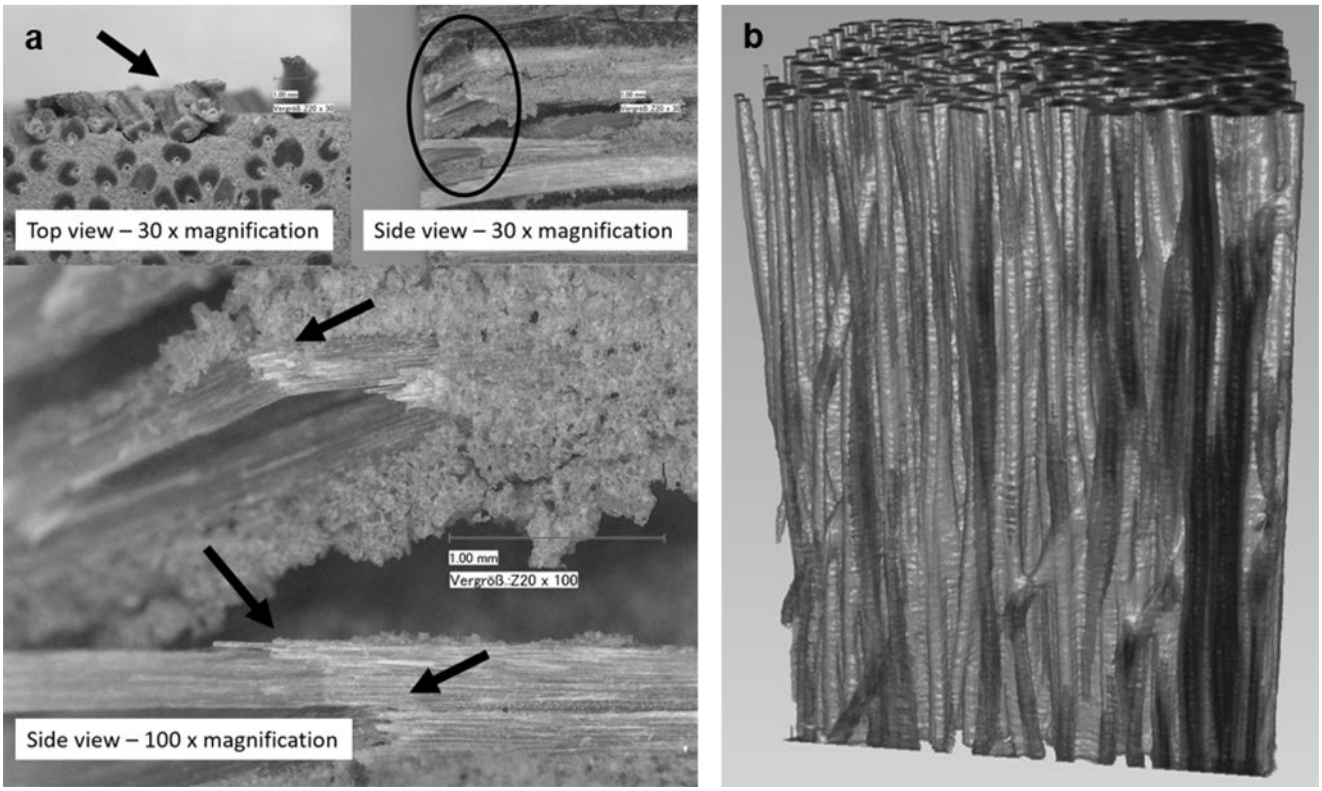


Fig. 11 **a** Micrograph of a compression test specimen after failure in 30-fold and 100-fold magnification over different views, failure of the vascular bundles marked with arrows; **b** 3D-reconstruction in ultra-high resolution (by Microtec´s Cube Eye Micro Computed Tomography Scanner) of the middle part of a tested longitudinal compression specimen (20 mm x 20 mm x 30 mm) with buckling failure of the vascular bundles

contains a low volume fraction of the reinforcement): the fibers can buckle out of phase relative to one another (symmetric about a line halfway between the fibers), (2) "shear mode" (if the volume fraction of the reinforcement is higher): the fibers buckle in phase with one another (antisymmetrically with respect to the line halfway between the fibers) and the matrix is subjected to shearing deformation. If fiber buckling occurs in the matrix, a column on an elastic foundation model would appear to be reasonable (Dow and Rosen 1965) and the buckle wavelength is directly proportional to the fiber diameter. Therefore, only a small influence of the specimen height on the compression strength II was found (Fig. 8a). It is assumed, that the exponent $>>1$ of the power law relationship of the compression strength can be explained with the cell wall thickening within the vascular bundles and its rising fiber cap diameter. The analysis to

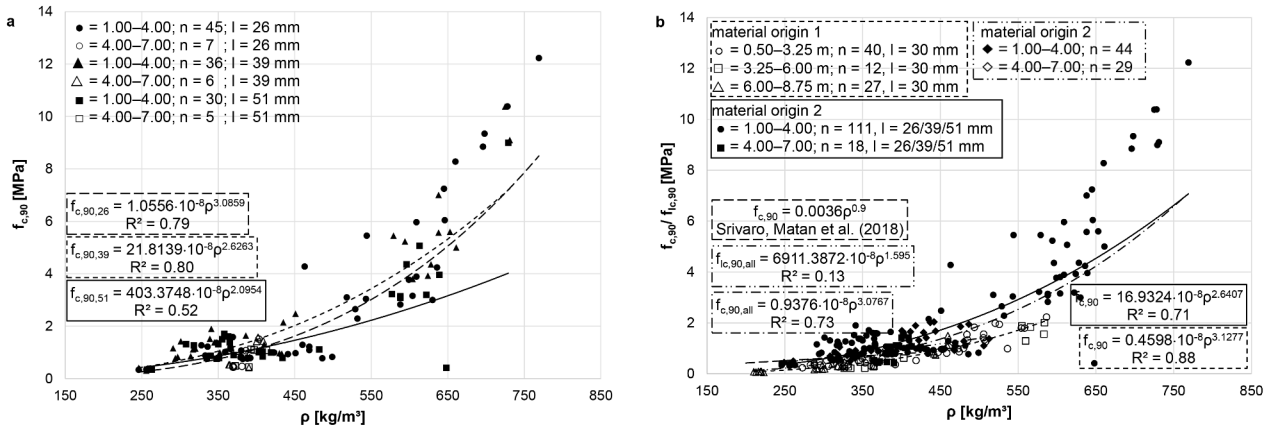


Fig. 12 Compression properties perpendicular to the vascular bundles plotted against the density (ρ); **a** proportional limit ($\mathbf{f}_{c,90}$) according to ISO 3132 (1975) for material origin 2 differentiated according to the specimen height and **b** proportional limit ($\mathbf{f}_{c,90}$) and locally compression strength ($\mathbf{f}_{lc,90}$) for both material origins

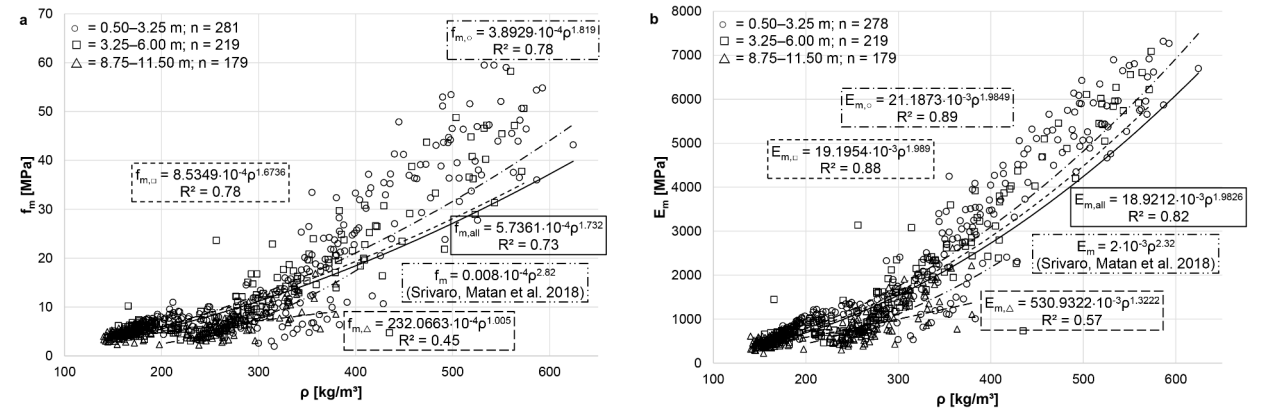


Fig. 13 Bending properties plotted against the density (ρ); **a** bending strength (f_m) and **b** bending modulus of elasticity (E_m)

find the fiber buckling load in each mode can be based on the energy method described by Greszczuk (1975). In addition to fiber buckling being caused by mechanical compressive loads, fiber buckling might also be caused by shrinkage stresses developed during drying the oil palm wood, which result from the matrix having a higher thermal coefficient of expansion than the fibers. Like for the tensile loading, the apparent Young´s modulus of the composite material in the direction of the fibers can be calculated according to the rule-of-mixtures (if the Young´s modulus of the parenchymatous ground tissue would be known) (Jones 1999). If the fiber modulus is assumed many times higher than the matrix modulus, the fiber modulus dominates the composite modulus.

In terms of structural performance, the specific compression strength ($M_4 = f_{c,0}/\rho$) parallel to the vascular bundles is shown in Table 3. Because of the power law relationship between compression strength and density, the performance index for minimum weight design by Ashby et al. (1995) calculated for oil palm wood rises with the density. Assumed densities between 200…600 kg/m³ for oil palm wood result in $M_4 = f_{c,0}/\rho = 20.3\ldots78.4$ MPa (Mg m^{-3})$^{-1}$. The strength-density performance indices (M_4 – M_6) of oil palm wood are comparable to that for coconut and date palm wood. For oil palm wood with higher densities they are in the range of small, clear plantation wood test specimens and structural size softwood (Table 3).

4.5 Compression tests perpendicular to the vascular bundles

The plot of the proportional limit for compression perpendicular to the vascular bundles ($f_{c,90}$) related to density is shown in Fig. 12. The values of the compression strength perpendicular to the vascular bundles ($f_{c,90}$, loaded over the entire specimen surface according to ISO 3132 (1975)) are dependent on the height within the trunk, range from 0.1 to 12.2 MPa and are comparable to those of Killmann and Lim

(1985) (2…3 MPa). At the same density, the compression strength perpendicular to the vascular bundles of material origin 1 are slightly lower than those of material origin 2 (Fig. 12b), but this effect may be due to the significantly higher proportion of test specimens from the upper trunk sections for material 1. The local compression strength perpendicular to the vascular bundles ($f_{lc,90,}$ loaded over 1/3 of the specimen surface according to ASTM D143 (2014)) ranges from 0.01…2.2 MPa and is comparable to that of Srivaro et al. (2018a) (0.4…1.2 MPa) (both determined at 2.5 mm deformation). Bigger test specimens show slightly lower compression strength ⊥ compared to smaller ones (Fig. 12a). Proportional limit ⊥ ($f_{c,90}$) increases with increasing density by the power law equation ($R^2 = 0.73$), the exponent is 3.0767. In contrast, the local compression strength ⊥ ($f_{lc,90}$) does not depend on the density ($R^2 = 0.13$) with a much lower exponent (1.595) of the power law equation, but is above that of Srivaro et al. (2018a) (0.9, because of their low density range, cf. Figure 12b). In comparison, common wood species show a modelled exponent of 2.0 (Easterling et al. 1982; Gibson and Ashby 1999), an experimentally derived exponent of 2.25 (Markwardt and Wilson 1935) and for softwoods 1.57 respectively for hardwoods 2.09 (Kretschmann 2010). The stress-strain curve of the compression test perpendicular to the vascular bundles shows the ductile behavior typical for wood and fiber-reinforced composites. A buckling failure of all the test specimens was observed macroscopically, microscopically the hard vascular bundles are released from the soft parenchyma.

4.6 Bending tests parallel to the vascular bundles

The plot of the bending strength (f_m) and the modulus of elasticity in bending (E_m) related to density is shown in Fig. 13. The values for f_m range from 2.0 to 59.5 MPa and are comparable to those of Lim and Gan (2005) (18.1…52.5…68.7 MPa for ρ = <350…350–500…>500 kg/m³), Erwinsyah (2008) (7.5…53.7 MPa) and Srivaro et al. (2018b) (7…58 MPa), in the range but with a much higher variance than those of Killmann and Lim (1985) (8…45 MPa) and Iswanto et al. (2010) (15.7…39.4 MPa), higher than those of Bakar et al. (1999), cit. in Fathi (2014) (6.6…28.9 MPa) and lower than those of Balfas (2006) (28.3…74.9 MPa for $\rho_{air-dry} = 330…670$ kg/m³) and Ratanawilai et al. (2006) (37.7…46.6 MPa for $\rho_{12} = 380…510$ kg/m³). The values of E_m range from 223 to 7,320 MPa and are comparable to those of Killmann and Lim (1985) (740…7,960 MPa), Balfas (2006) (3,219…8,596 MPa for $\rho_{air-dry} = 330…670$ kg/m³), Ratanawilai et al. (2006) (5,268…2,845 MPa for $\rho_{12} = 380…510$ kg/m³), Erwinsyah (2008) (928…6,869 MPa) and Srivaro et al. (2018b) (500…7,000 MPa), in the range but with a much higher variance than those of Lim and Gan (2005) (1,712…5,094…6,744 MPa for ρ = <350…350–500…>500 kg/m³) and Iswanto et al. (2010) (1,891…4,508 MPa) and higher than those of Bakar et al. (1999), cit. in Fathi (2014) (285…3,168 MPa). Bending strength and MOE increase with increasing density by the power law equation ($R^2 = 0.73$ respectively $R^2 = 0.82$). The exponent for f_m is 1.732 and comparable to those of Srivaro et al. (2018b) for oil palm wood (1.92) and Rich (1987b) as a pooled value for six species of arborescent palms in the lowland rain forest of Costa Rica (2.05), lower than that of Srivaro et al. (2018a) for oil palm wood (2.82) and higher than that for common wood species (experimental derived exponent 1.25 (Markwardt and Wilson 1935) and for softwoods 1.01 respective for hardwoods 1.13 (Kretschmann 2010). The exponent for E_m is 1.9826 and comparable to those of oil palm wood by Srivaro et al. (2018b) (1.88) and Srivaro et al. (2018a) (2.32) and the pooled value for six species of arborescent palms in the lowland rain forest of Costa Rica (2.46) by Rich (1987b), but much higher than that for common wood species (experimentally derived

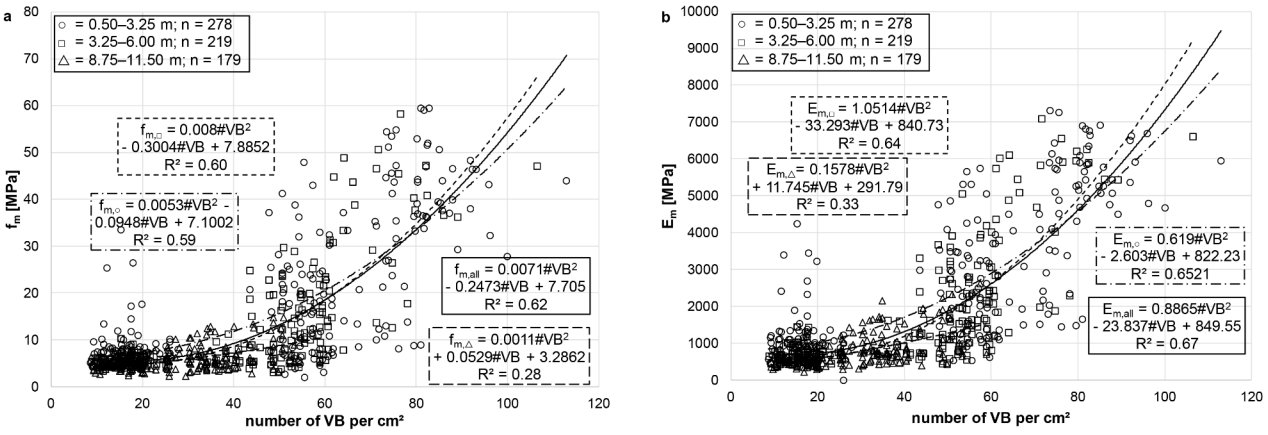


Fig. 14 Bending properties plotted against the number of vascular bundles per unit area (#VB); **a** bending strength (f_m) and **b** bending modulus of elasticity (E_m)

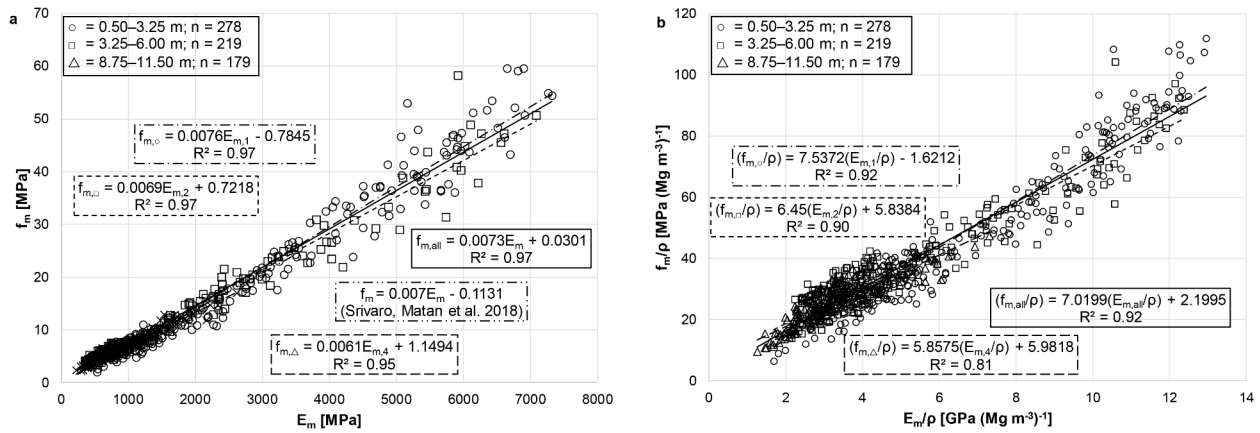


Fig. 15 Relationship between bending strength (f_m) and stiffness (E_m) parallel to the vascular bundles; **a** absolute values and **b** performance indices

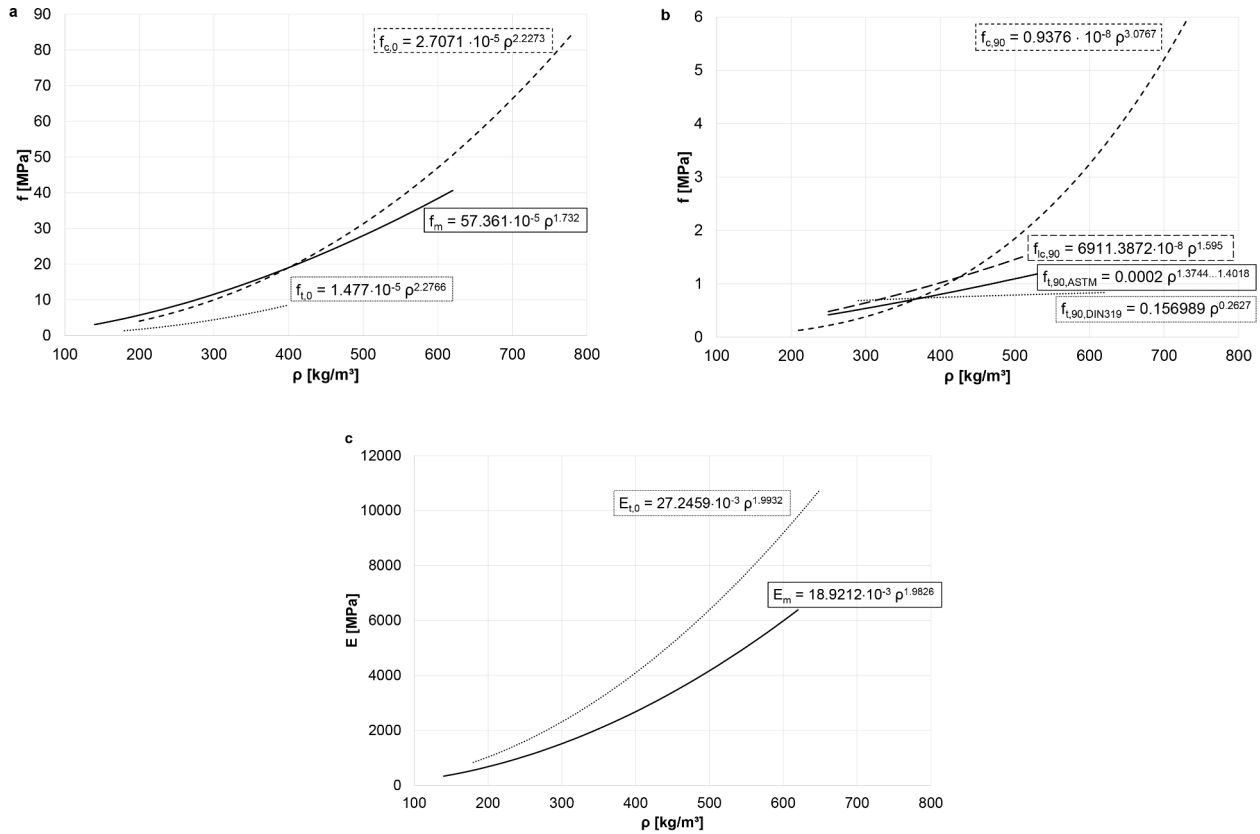


Fig. 16 Various properties plotted against the density (ρ); **a** various strength parallel to the vascular bundles (f_0), **b** various strength perpendicular to the vascular bundles (f_{90}) and **c** various modulus of elasticity (E)

exponent 1.0 (Markwardt and Wilson 1935) and for softwoods 0.84, respectively for hardwoods 0.7 (Kretschmann 2010). Deviant from Srivaro et al. (2018a) an influence of the trunk height can be observed (Figs. 13 and 14). The number of vascular bundles per area shows much lower correlation to the bending MOR and MOE (Fig. 14) than the density (Fig. 13). Figure 15a shows that f_m seems to be strongly related to E_m, showing relatively high $R^2 = 0.97$ (without influence of the trunk height), which indicates that f_m can be predicted from the known E_m value independent of the trunk height. In terms of structural performance, the specific bending strength (f_m/ρ) and modulus of elasticity (E_m/ρ) parallel to the vascular bundles should be considered, shown in Fig. 15b.

The stress-strain curve of the bending test parallel to the vascular bundles with higher density especially in the lower trunk heights shows brittle rupture with only little prior change in the rate of deformation (low nonlinear), which is typical for softwoods and hardwoods. However – different from common wood species – the test specimens with lower density especially in the upper trunk show ductile behavior and no fracture, which is not typical for bending test of wood (Bodig and Jayne 1982).

4.7 Relationship between macro- and micromechanical behavior

Figure 16a shows the tensile, compressive and bending strength of oil palm wood as a function of density. The compressive strength parallel to the vascular bundles ($f_{c,0}$) is around 1.4 times the tensile strength parallel ($f_{t,0}$). In contrast, softwoods and hardwoods show a reversed ratio for small, clear test specimens (ratio between compressive and tensile strength parallel to the grain of 1:2 according to Bosshard (1984) and 1:1.9 according to Niemz and Sonderegger (2003)). The low tensile strength of oil palm wood in this study might be due to the angle between the direction of the vascular bundles and the direction of the applied tensile stress in the tensile test specimens, which results in tensile strength values that are measured too low. However, because of the helical orientation of the bundles with deviations in radial direction (Tomlinson 1990; Rueggeberg et al. 2008, 2009; González and Nguyen 2016), it is not possible to process small (that regular spaced vascular bundles) test specimens with perfectly aligned vascular bundles along the axis of the test specimen. The ratio of compression strength parallel (Fig. 16a) and perpendicular to the vascular bundles (Fig. 16b) is 37.1–11.8 : 1 within the density range relevant for oil palm wood ($\rho = 200 \ldots 650$ kg/m³) and therefore much higher than for clear wood in compression with 10:1 according to Bodig and Jayne (1982). Figure 16c shows the Young´s modulus in tension and the MOE in bending. It can be observed that for oil palm wood $E_{t,0} : E_m = 1.5 : 1$. This is in accordance with Egner (1957) for common wood species, who stated that $E_{t,0} > E_m$, and slightly above Kretschmann

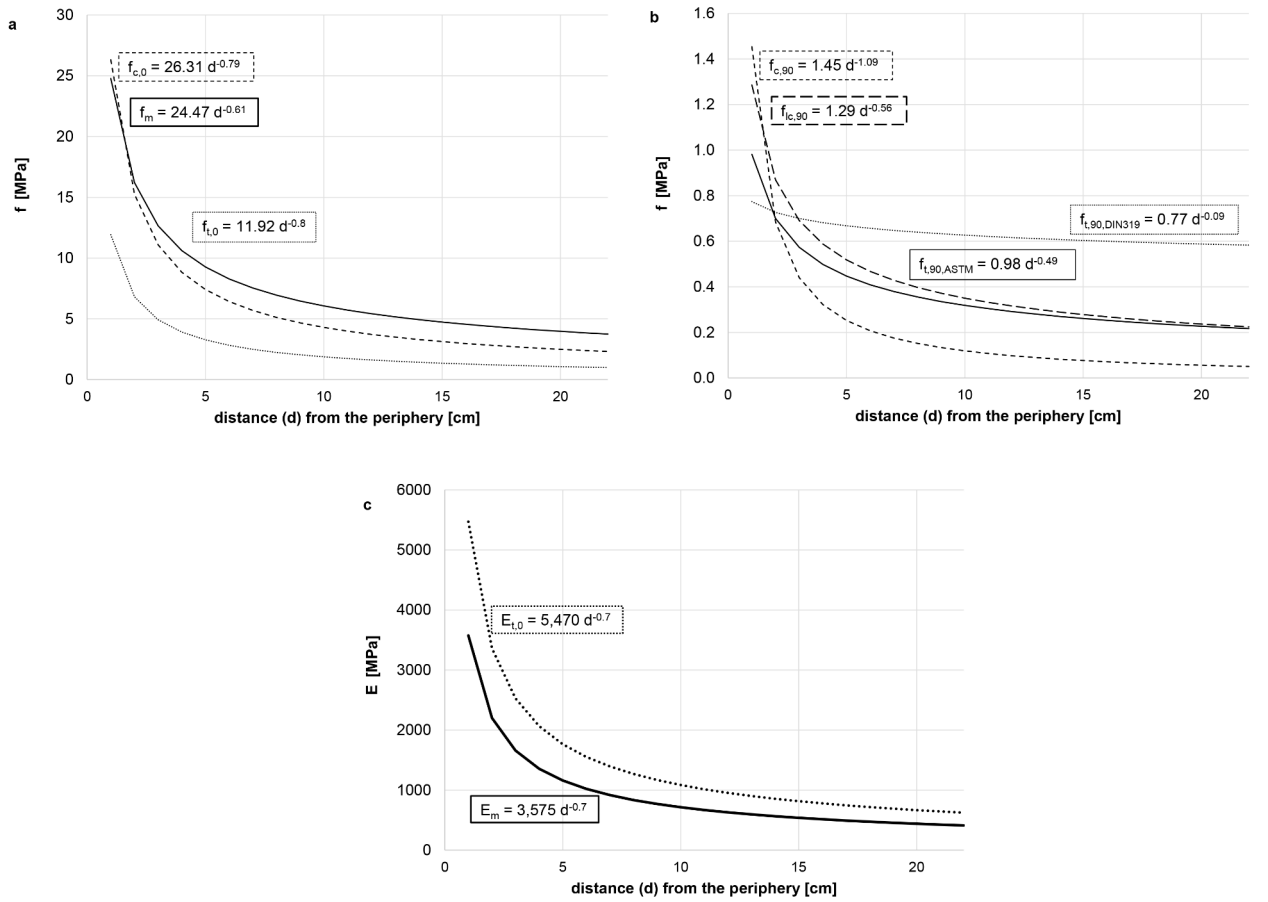


Fig. 17 Various properties plotted against the distance from the periphery (d); **a** various strength parallel to the vascular bundles (f_0), **b** various strength perpendicular to the vascular bundles (f_{90}) and **c** various modulus of elasticity (E). Distance from periphery excludes the "bark" of the oil palm trunk

(2010), who stated that E_m includes an effect of shear deflection and therefore can be increased by 10%.

Compared to dicotyledons, all strength values show a high correlation with the stiffnesses (absolute and specific). This is caused by the very large density range of the oil palm wood test specimens and the therefore large range of property values compared to those of dicotyledons. Strength can be predicted from stiffness. All strength and stiffness values increase with the density as power law relationships with similar exponents; this corresponds to the results for oil palm wood according to Srivaro et al. (2018a, b) and for other palm species according to Rich (1987b), but the determined exponents are very different from those of softwood and hardwood species from modelling (Easterling et al. 1982; Gibson and Ashby 1999; Price 1929) or experimental results (Bodig and Goodman 1973; Kretschmann 2010; Markwardt and Wilson 1935). This might be due to the different anatomical structures: dicotyledons consist of a honeycomb-like structure of tracheid (softwoods) or fiber cells (hardwoods), while monocotyledonous palms tissues are made up of vascular bundles (having honeycomb-like prismatic cells and dense fibers aligned along the stem) surrounded by parenchymatous ground tissue (made up of thin-walled polyhedral parenchyma like closed cell foam-like structure) (Gibson 2012). Palms have a more heterogeneous structure in comparison to dicotyledons. The adapted rule of mixture based on the number of vascular bundles per unit area is confirmed for the density (Fig. 2). But tensile Young´s modulus and strength parallel increase with the density as a power law relationship with exponents > 1 (Fig. 16a + c); therefore, the adapted rule of mixture directly based on the density and indirectly via the relationship between density and number of vascular bundles per unit area also for the number of vascular bundles per unit area cannot be confirmed by the results. Some of the assumed basic restrictions for composite materials in Chap. 1 can be confirmed (composite is initially stress free, linearly elastic, macroscopically homogeneous and orthotropic; vascular bundles are linear elastic (Fathi 2014), parenchymatous ground tissue is homogeneous and isotropic (Gibson 2012), some are still unclear (is the parenchymatous ground tissue linear elastic and void free? And are the vascular bundles perfectly bonded?); some have to be denied (vascular bundles are not homogeneous (Fathi 2014), not isotropic (Gibson 2012), not regularly spaced, not perfectly aligned (cf. helical course in Chap. 1)). The concentration of vascular bundles, as well as the concentration of fibers within the bundles, is greater in the periphery of the trunk than in the central tissue (Fathi 2014; Lim and Khoo 1986). Cell wall thickening is more pronounced in the peripheral tissue than in the central tissue and more at the bottom of the trunk than at the top of the trunk (Rich 1987a), because the bending stresses on the arborescent palm stem are greatest on the bottom at the periphery. Furthermore, the cell wall properties themselves are not constant, but differ in cells of different densities. Cell wall thickening means that as the palm tissue (vascular bundles and parenchymatous ground tissue) ages more cell wall layers are added on the cell wall towards the lumen of the cells resulting in smaller lumina diameters and thicker cell walls containing a higher cellulose content (Lim and Khoo 1986). The density in the peripheral zones at the bottom of the trunk rises over time because the trunk volume increase is lower than the mass increase by added volume of additional cell wall layers. However, the density increase due to cell wall thickening is lower than the increase of the elastomechanical properties, which leads to exponents > 1 of the power law relationship and therefore leads to the rejection of the adapted rule of mixture for the tensile Young´s modulus and tensile strength parallel to the vascular bundles in this study. When analyzing or calculating the rule of mixture, it is essential to take into account that the elastic modulus and ultimate tensile strength of the vascular bundles and the parenchymatous ground tissue depend on the age of the palm and the position within the trunk. Because of a percentage related higher increase of density and elastomechanical properties due to cell wall thickening in the parenchymatous ground tissue compared to the vascular bundles, the exponent of the compression strength perpendicular (mainly matrix dominated) is higher than that parallel to the vascular bundles (mainly vascular bundle dominated).

The power law relationships of the strength respectively modulus properties and the density in Fig. 16 in combination with the power function of density and distance (d) from the periphery of the trunks $\rho_{mean} = 462.41\ d^{-0.353}$ by Fruehwald-Koenig et al. (n.d., in submission) leads to the apparent properties depending on the position in the cross section shown in Fig. 17. It shows a dramatic drop in strength and stiffness within the first 2.5 cm from the periphery, which requires an adapted primary processing of the trunks and secondary processing of the lumber.

In contrast to the results of Srivaro et al. (2018a), who only investigated the lower 5 m of the trunk with mainly low density specimens, and according to the results of Fathi (2014), all mechanical properties depend on the height within the trunk; “useful and competitive” mechanical properties for common type products can only be found in the lower approximately 6 m trunk section. Note, that the results may be influenced by the non-uniform distribution of the specimens tested over the stem height and stem cross section. The elastomechanical properties are not only influenced by the density and the location within the trunk (height and cross section) as shown in this study, but probably also by the age of the palm, the oil palm subspecies

and differences between individual palms (not inverstigated in this study) and the plantation sites. In the context of this investigation, no clear difference is determined in the compressive strength II and ⊥ ($f_{c,0}$, $f_{c,90}$) as well as the tensile properties II ($f_{t,0}$, $E_{t,0}$) for the two material origins (both from Johor, South Peninsular Malaysia). Therefore, a multivariate regression model with all potential influencing factors should be calculated. This, however, is difficult due to the very large number of specimens necessary and the limited amount of oil palm material available in laboratories.

Rittiphet et al. (2021) demonstrated that pre-treating oil palm wood through water impregnation, followed by subsequent freezing below − 10 °C, induces microcracks between parenchyma cells. This pre-treatment allows for defect-free drying, even under severe conditions with temperatures reaching 200 °C, in contrast to untreated reference specimens, which exhibit substantial cell collapse with internal voids and irregular shrinkage. In this study, material from origin 1 underwent freezing at -10 °C for several weeks before kiln drying, while material from origin 2 did not undergo freezing. Both sets of lumber were kiln-dried at temperatures significantly below 100 °C. However, some individual boards from both origins exhibited signs of defects after kiln drying, preventing the production of test specimens from these boards. Potential microcracks on test specimens cannot be dismissed, attributed to freezing and/or kiln drying for origin 1 and solely kiln drying for origin 2. Microcracks between parenchyma cells and at the interface of parenchyma cells and vascular bundles might impact shear properties (beyond the scope of this paper) and compressive properties perpendicular to vascular bundles, as both are influenced by the properties of the parenchymatic ground tissue. For the compressive strength perpendicular to the vascular bundles, slightly lower strength values at the same density cannot be excluded for material 1 (Fig. 12b), but this may also be due to the significantly higher proportion of test specimens from the upper trunk sections for material 1. No difference between the two material origins was found for the compressive strength parallel to vascular bundles ($f_{c,0}$) in Fig. 8 and the tensile properties parallel ($f_{t,0}$, $E_{t,0}$) in Fig. 3. However, as discussed above, compressive and tensile properties parallel, as well as flexural properties, depend mainly on the vascular bundle properties or the interaction of the properties of vascular bundles and parenchymatic ground tissue. Consequently, these properties are presumed to be less affected by potentially occurring and undetected microcracks between parenchyma cells resulting from freezing or kiln drying. Thus, it is posited that the differential pre-treatment of material 1 and 2 concerning freezing has minimal or negligible effects on tensile, compressive, and flexural properties parallel to vascular bundles. Further investigation is warranted to explore the influence of microcracks arising from freezing and/or kiln drying on compressive properties perpendicular to vascular bundles.

Because of the power law relationship between strength, respectively stiffness and density, the performance indices for minimum weight design by Ashby et al. (1995) calculated for oil palm wood rise with the density and are shown for assumed densities between 200…600 kg/m³ in Table 3. They are comparable to that for coconut and date palm wood. The modulus-density performance index M_1 (tie under uniaxial load) is lower, whereas M_2 (beam in flexure) and M_3 (plate in flexure) are comparable to that of structural size softwood lamellas. The strength-density performance indices (M_4 – M_6) of oil palm wood with higher densities determined by compression tests are in the range of small, clear plantation wood test specimens and structural size softwood. In contrast, M_4 – M_6 of oil palm wood based on tensile tests is much lower than that of small, clear plantation wood test specimens, high-density oil palm wood is in the range of low grade softwood lamellas of structural size. The performance index for elastic design M_8 to allow large, recoverable deformation based on tensile tests is lower than that from small, clear plantation wood test specimens, but in the range of structural size softwood lamellas.

5 Conclusion

The study reveals crucial insights into the elastomechanical properties of oil palm wood, highlighting both similarities and differences with common wood species. The tensile and compression properties parallel and perpendicular to the vascular bundles, and bending properties are described as a function of density and position within the trunk, showing significant relationships between these properties. Because the adapted rule-of-mixture based on the number of vascular bundles per unit area is confirmed for the density, the density is sufficient for grading elastomechanical properties, making it unnecessary to determine the number of vascular bundles for strength grading. The compression strength parallel to the vascular bundles ($f_{c,0}$) is approximately 1.4 times the tensile strength parallel ($f_{t,0}$), a reversal from typical softwood and hardwood ratios on small, clear test specimens. This discrepancy is likely due to the helical orientation of the vascular bundles, which complicates specimen alignment and may underestimate tensile strength. The compression strength ratio parallel and perpendicular to vascular bundles is much higher for oil palm wood compared to common wood species, as the perpendicular compression strength is very low. The Young´s modulus in tension ($E_{t,0}$) is approximately 1.5 times the MOE in bending (E_m), similar to common wood species.

The research confirms a strong correlation between strength respectively stiffness and density, following power law relationships with exponents greater than one. This aligns with previous studies on oil palm wood and other palm species but diverges from patterns in softwoods and hardwoods. Therefore, the adapted rule of mixtures for the tensile Young´s modulus and tensile strength parallel to the vascular bundles is rejected, because the number of vascular bundles per unit area, the share of fibers within the bundles and the cell wall thickening over time is not constant over the entire trunk. This emphasizes the need to consider the age as well as height and cross-sectional location within the trunk when analyzing the elastomechanical properties and optimizing the processing and utilization of oil palm wood in various applications. For example, only the lower 5 to 6 m should be used for solid wood-based products and these should be cut into at least two trunk sections. Further studies should consider multivariate regression models to account for additional influencing factors, such as palm age, subspecies, and plantation sites, to refine these findings and expand their applicability.

Oil palm wood availability offers good opportunities to supplement or substitute common tropical timber species, especially in Asia, and from pine plantations. The material shows promising potential especially as a plate material. Its performance indices for minimum weight design, comparable to coconut and date palm wood, indicate that the modulus-density indices for beam and plate in flexure (M_2 and M_3) are similar to those of structural softwood lamellas. The strength-density indices (M_4 – M_6) for higher-density oil palm wood in compression are on par with small, clear plantation wood test specimens and structural size softwood. However, the tensile strength-density indices for oil palm wood are lower, placing high-density oil palm wood in the range of low-grade structural softwood lamellas.

Given the unique unidirectional long-fiber-reinforced bio-composite structure oil palm wood, special product development (including material respectively product modeling) and process technology development is necessary for market competitiveness. To obtain predictable and uniform product properties, lumber must be separated lengthwise by required density in dense-homogeneous strips, graded into density classes, and then reassembled into products. Since all strengths highly correlate with stiffness, the modulus of elasticity can be used for strength grading. Considering the uniform structure and absence of knots in palm wood, larger glued structural members may have very similar properties to those of small specimens, as confirmed by initial bending, compression and tensile tests. Unlike common wood species, palm wood´s structural member might not suffer from significantly lower properties due to knots. Because of the high coefficient of variation (CV) in oil palm wood compared to common wood species, grading by density is mandatory as most design values are based on the 5th percentile, and high CVs result in low product performance. It is crucial to test palm timber in product-size, glued specimens. For load bearing products, challenges include grading and trimming of the lumber, properties of full-size members, long-term durability under load and wet climate, and design values as well as standardization to match building codes.

Acknowledgements The oil palm material was made available by the German Federal Ministry of Education and Research through the "KMU-innovativ" project "Technologies for Lumber Processing from Oil Palm Trunks (02PK2458)", project coordinator: Simon Möhringer Anlagenbau GmbH, Wiesentheid, Germany, and University of Hamburg, Institute for Wood Science, by the Deutsche Investitions- und Entwicklungsgesellschaft (DEG) through the project "Effiziente Nutzung von Oil Palm Trunks in Asien", project coordinator: Palmwood-Net, Detmold, Germany as well as by the German Federal Ministry of Education and Research through the "Bioökonomie International 2017" project "Oilpalmsugar (031B0767A)", project coordinator: Ostwestfalen-Lippe University Applied Sciences and Arts. The generation of the raw data of the bending test was in the context of the Bachelor Thesis of M.Sc. Matthias Schuff. The locally compression test ⊥ and the tensile test ⊥ according to ASTM D 143 (2014) was in the context of the Bachelor Thesis of B.Eng. Lukas Blumenstein. The compression and tensile tests on test specimen from the second material origin were in the context of the scientific internship of M.Sc. Lena Reinhardt. Many thanks for their permission to use the raw data. The authors would also like to thank Microtec Company for the 3D-reconstruction of test specimen in ultra-high resolution with the Cube Eye Micro Computed Tomography Scanner.

Author contributions Lena Heister performed the measurements and analyses of the compression and tensile tests (fc,0; fc,90 and ft,0) on test specimen from the first material origin close to Kluang, Malaysia according to DIN 52185 (1976), DIN 52192 (1979), DIN 52188 (1979) and DIN 319 (1993 (D)). Katja Fruehwald-Koenig had the idea, supervised students, who did the laboratory testing, made and reviewed the analyses, worked on the theoretical background and the material modelling and wrote solely the paper.

Funding Open Access funding enabled and organized by Projekt DEAL.

Data Availability The data that support the findings of this study are available from the corresponding author, Katja Fruehwald-Koenig,upon reasonable request.

Declarations

Competing interests The authors declare no competing interests.

Open Access This article is licensed under a Creative Commons Attribution 4.0 International License, which permits use, sharing, adaptation, distribution and reproduction in any medium or format, as long as you give appropriate credit to the original author(s) and the source, provide a link to the Creative Commons licence, and indicate if changes were made. The images or other third party material in this article are included in the article's Creative Commons licence, unless indicated otherwise in a credit line to the material. If material is not

included in the article's Creative Commons licence and your intended use is not permitted by statutory regulation or exceeds the permitted use, you will need to obtain permission directly from the copyright holder. To view a copy of this licence, visit http://creativecommons.org/licenses/by/4.0/.

References

Ashby MF, Gibson L, Wegst U, Olive R (1995) The mechanical properties of natural materials. I. Material property charts. Proc R Soc Lond A 450:123–140. https://doi.org/10.1098/rspa.1995.0075

ASTM D143 (2014) Standard Test Methods for Small Clear Specimens of Timber

Bakar E, Rachman O, Darmawan W, Hidayat I (1999) Utilization of oil palm trees as building and furniture materials (2): mechanical properties of oil palm trunk. J for Prod Technol 12:10–20

Bakar ES, Sahri MH, H'ng P (2008) Anatomical characteristics and utilization of oil palm wood. In: Nobuchi T, Sahri MH (ed) The formation of wood in tropical forest trees - a challenge from the perspective of functional wood anatomy. UPM, pp 161–178

Bakar BFA, Tahir PM, Karimi A, Bakar ES, Uyup MKA, Choo ACY (2013) Evaluations of some physical properties for oil palm as alternative biomass resources. Wood Mater Sci Eng 8:119–128. https://doi.org/10.1080/17480272.2012.701666

Balfas J (2006) New Approach to oil palm wood utilization for woodworking production part 1: Basic properties. Indonesian J Forestry Res 3:55–65. https://doi.org/10.20886/ijfr.2006.3.1.55-65

Bodig J, Goodman JR (1973) Prediction of elastic parameters of wood. Wood Sci 5:249–264

Bodig J, Jayne BA (1982) Mechanics of wood and wood composites. Van Nostrand Reinhold Company, New York

Bolza E, Kloot NH (1966) The mechanical properties of 81 New Guinea timbers. Commonwealth Scientific and Industrial Research Organization, Australia

Bosshard HH (1984) Holzkunde - Zur Biologie, Physik und Chemie des Holzes - Band 2 (Wood science - The biology, physics and chemistry of wood - Volume 2). 2. Auflage. Birkhäuser Verlag, Basel und Stuttgart

Darwis A, Nurrochmat DR, Massijaya MY, Nugroho N, Alamsyah EM, Bahtiar ET, Safe´i R (2013) Vascular bundle distribution effect on density and mechanical properties of oil palm trunk. Asian J Plant Sci 12:208–213. https://doi.org/10.3923/ajps.2013.208.213

DIN 50014 (2018) Normalklimate für Vorbehandlung und/oder Prüfung - Festlegungen (Standard atmospheres for conditioning and/or testing — Specifications). Beuth, Berlin

DIN 52182 (1976) Prüfung von Holz - Bestimmung der Rohdichte (Testing of wood; determination of density). Beuth, Berlin

DIN 52185 (1976) Bestimmung der Druckfestigkeit parallel zur Faser (Testing of wood; compression test parallel to grain). Beuth, Berlin

DIN 52186 (1978) Prüfung von Holz - Biegeversuch (Testing of wood; bending test). Beuth, Berlin

DIN 52188 (1979) Prüfung von Holz; Bestimmung der Zugfestigkeit parallel zur Faser (Testing of wood; determination of ultimate tensile stress parallel to grain). Beuth, Berlin

DIN 52192 (1979) Druckversuch quer zur Faserrichtung (Testing of wood; compression test perpendicular to grain). Beuth, Berlin

DIN 68364 (2003) Kennwerte von Holzarten (Properties of wood species — density, modulus of elasticity and strength). Beuth, Berlin

Dow NF, Gruntfest IJ (1960) Determination of most needed potentially possible improvements in materials for ballistic and space vehicles. 4. General Electric Company, Air Force Contract AF, 647

Dow NF, Rosen BW (1965) Evaluations of Filament-Reinforced composites for Aerospace Structural Applications. General Electric Co Philadelphia, PA

Easterling K, Harrysson R, Gibson L, Ashby MF (1982) On the mechanics of balsa and other woods. Proc R Soc Lond A 383:31–41. https://doi.org/10.1098/rspa.1982.0118

Egner K (1957) Bestimmung der Elastizität der Hölzer (Determination of the elasticity of woods). In: Graf O (ed) Die Prüfung nichtmetallischer Baustoffe (The testing of non-metallic building materials). 2. verbesserte Auflage. Springer-Verlag, Berlin, Göttingen, Heidelberg, pp 89–92

Elkhal M, Hakam A, Ez-Zahraouy H, Hader A, Tanasehte M, Ziani M (2022) Mechanical and physical properties of the date palm stem (*Phoenix dactylifera* L.) in Morocco. Eur. J. Wood Prod. 80:693–703. https://doi.org/10.1007/s00107-021-01777-0

EN 338 (2016 (D)) Structural timber - strength classes. European Committee for Standardization (CEN), Brussels

EN 319 (1993 (D)) Particleboards and fibreboards; determination of tensile strength perpendicular to the plane of the board. European Committee for Standardization (CEN), Brussels

Erwinsyah SH (2008) Improvement of Oil Palm Wood Properties Using Bioresin. Dissertation, Technische Universität Dresden

FAO (2024) Area harvested of oil palm fruits worldwide in 2022. Food and Agriculture Organization of the United Nations, Rome

Fathi L (2014) Structural and Mechanical Properties of the Wood from Coconut Palms, Oil Palms and Date Palms. Dissertation, University of Hamburg

Fruehwald A, Koelli N (2019) Oil palm plantations and oil palm timber availability. In: Handbook oil palm wood utilization, vol 1. Hamburg

Gan K, Choo K, Lim S (2001) Basic density and moisture content distributions in 30-year-old oil palm (Elaeis guineensis) stems. J Trop for Prod 7:184–191

Gibson LJ (2012) The hierarchical structure and mechanics of plant materials. J R Soc Interface 9:2749–2766. https://doi.org/10.1098/rsif.2012.0341

Gibson LJ, Ashby MF (1999) Cellular solids: structure and properties, 2 edn. Cambridge University Press, Camebridge, UK

Gibson LJ, Ashby MF, Harley BA (2010) Cellular materials in nature and medicine. Cambridge University Press, New York

González OM, Nguyen KA (2016) Cocowood fibrovascular tissue system - another wonder of plant evolution. Front Plant Sci 7:1141. https://doi.org/10.3389/fpls.2016.01141

Greszczuk L (1975) Microbuckling failure of circular fiber-reinforced composites. AIAA J 13:1311–1318. https://doi.org/10.2514/3.60544

Harnisch J (2016) Untersuchungen zum Trocknungsverhalten von Ölpalmen-Schnittholz (Studies on the Drying Behavior of Oil Palm Lumber). MSc-Thesis, University of Hamburg

ISO 3132 (1975) Wood - Testing in compression perpendicular to grain. International Organization for Standardization

Iswanto A, Sucipto T, Azhar I, Coto Z, Febrianto F (2010) Physical and Mechanical Properties of Palm Oil Trunk from Aek Pancur Farming-North Sumatera. Jurnal Ilmu Dan Teknologi Hasil Hutan 3:1–7

Jones RM (1999) Mechanics of composite materials, 2 edn. Taylor & Francis Group, New York

Jumaat MZ, Rahim AHA, Othman J, Midon MS (2006) Strength evaluation of oil palm stem trussed rafters. Constr Build Mater 20:812–818. https://doi.org/10.1016/j.conbuildmat.2005.01.049

Karlinasari L, Ritonga RP, Maddu A (2019) Prediction of Bending and Hardness Strength Properties of Oil Palm (Elaeis guineensis Jacq.) Trunk using Nondestructive Evaluation of Ultrasonic Testing Method. Paper presented at the 21st International Nondestructive Testing and Evaluation of Wood Symposium, Freiburg, Germany, 24.-27.09.2019

Kelly A, Davies G (1965) The principles of the fibre reinforcement of metals. Metall Reviews 10:1–77. https://doi.org/10.1179/mtlr.1965.10.1.1

Killmann W, Lim SC (1985) Anatomy and Properties of Oil Palm Stem. Paper presented at the National Symposium of Oil Palm By-Products, Kuala Lumpur, Malaysia

Kipp D (2022) Untersuchung verschiedener Dehnungsmessmethoden für die Bestimmung des Druck-E-Moduls an Vollholzproben (Investigation of Various Strain Measurement Methods for the Determination of the Compression Modulus of Elasticity in Solid Wood Samples). BSc-Thesis, Ostwestfalen-Lippe University of Applied Sciences and Arts

Koelli N (2016) Density and Moisture Distribution in Oil Palm Trunks from Peninsular Malaysia. BSc-Thesis, University of Hamburg

Koelli N (2018) Einfluss des Schneidenverschleißes von Zerspanungswerkzeugen auf die Klebefestigkeit von Ölpalmenholz (Influence of Cutting Tool Wear on the Adhesive Strength of Oil Palm Wood). MSc-Thesis, University of Hamburg

Kretschmann DE (2010) Chap. 5: Mechanical Properties of Wood. In: U. S. Department of Agriculture / Forest Service / Forest Products Laboratory (ed) Wood Handbook - Wood as an Engineering Material. General Technical Report FPL-GTR-190. U.S. Department of Agriculture, Madison, WI, p 509

Lim S, Fujii T (1997) A note on the structure of oil palm trunk by scanning electron microscopy. J Trop for Prod 3:105–109

Lim SC, Gan K (2005) Characteristics and utilization of oil palm stem. Timber Bull 35

Lim S, Khoo K (1986) Characteristics of oil palm trunk and its utilization. Malaysian Forester 49:3–22

Markwardt LJ, Wilson TRC (1935) Strength and related properties of woods grown in the United States, vol 479. US Government Printing Office, Washington D.C.

Niemz P, Sonderegger W (2003) Untersuchungen zur Korrelation ausgewählter Holzeigenschaften untereinander und mit der Rohdichte unter Verwendung von 103 Holzarten (Studies on the correlation of selected wood properties with each other and with density using 103 wood species). Schweiz Z Forstw 154:489–493

Peh T, Khoo K (1984) Timber properties of Acacia mangium, Gmelina arborea,[and] Paraserianthes [Albizia] falcataria and their utilization aspects. Malaysian Forester 47:285–303

Price A (1929) I. A mathematical discussion on the structure of wood in relation to its elastic properties. Phil Trans R Soc Lond A 228:1–62

Ratanawilai T, Chumthong T, Kirdkong S (2006) An investigation on the mechanical properties of trunks of palm oil trees for the furniture industry. J Oil Palm Res 18:114–121

Rich PM (1987a) Developmental anatomy of the stem of Welfia Georgii, Iriartea gigantea, and other arborescent palms: implications for mechanical support. Am J Bot 74:792–802. https://doi.org/10.2307/2443860

Rich PM (1987b) Mechanical structure of the stem of arborescent palms. Bot Gaz 148:42–50. https://doi.org/10.1086/337626

Rittiphet C, Dumyang K, Matan N (2021) Effect of pre-mechanical compression on free water removal, drying collapses and associated internal voids of oil palm wood. Eur. J. Wood Prod. 79, 925–940. https://doi.org/10.1007/s00107-021-01674-6

Rosen BW (1964) Tensile failure of fibrous composites. AIAA J 2:1985–1991. https://doi.org/10.2514/3.2699

Rueggeberg M, Speck T, Paris O, Lapierre C, Pollet B, Koch G, Burgert I (2008) Stiffness gradients in vascular bundles of the palm Washingtonia robusta. Proc Royal Soc Lond B: Biol Sci 275:2221–2229. https://doi.org/10.1098/rspb.2008.0531

Rueggeberg M, Speck T, Burgert I (2009) Structure–function relationships of different vascular bundle types in the stem of the Mexican fanpalm (Washingtonia robusta). New Phytol 182:443–450. https://doi.org/10.1111/j.1469-8137.2008.02759.x

Shao Z, Wang F (2018) Fracture mechanics of plant materials. Springer, Singapore

Srivaro S, Matan N, Lam F (2018a) Property gradients in oil palm trunk (Elaeis guineensis). J Wood Sci 64:709–719. https://doi.org/10.1007/s10086-018-1750-8

Srivaro S, Rattanarat J, Noothong P (2018b) Comparison of the anatomical characteristics and physical and mechanical properties of oil palm and bamboo trunks. J Wood Sci 64:186–192. https://doi.org/10.1007/s10086-017-1687-3

Srivaro S, Cherdchim B, Pasztory Z (2019) Bending and Compressive properties of Finger-jointed oil. Palm Wood Prod BioResources 14:6341–6352

Sulaiman O, Fahmi Awalludin M, Hashim R, Mondal MIH (2012) The effect of relative humidity on the physical and mechanical properties of oil palm trunk and rubberwood. Cellulose Chem Technol 46:401–407

Sulc VK (1985) Mechanical properties of coconut palm wood. Zamboanga, Philippines

Tan YK (1979) The properties of Acacia mangium from Sabah Research Plantation. Timber Research and Technical Training Centre, Forest Department, Sarawak, Malaysia

Tomlinson PB (1990) The structural biology of palms. Oxford University Press, Oxford

Tufashi T (2013) Physical-Mechanical and Chemical Properties of the Wood of Oil palm and Date palm Trees. BSc-Thesis, University of Hamburg

Wagenfuehr R (2000) Holzatlas (Wood Atlas). vol 5. ergänzte und erweiterte Auflage. Fachbuchverlag Leipzig im Carl Hanser Verlag

Publisher's Note Springer Nature remains neutral with regard to jurisdictional claims in published maps and institutional affiliations.